Design and Measurement of the Silicon Slab Optical Waveguide

Dissertation

Design and Measurement of the Silicon Slab Optical Waveguide

シリコンスラブ光導波路の設計と測定

Graduated School of
Natural Science & Technology
Kanazawa University

Division of
Electrical Engineering &
Computer Science

Student ID. No. 1724042003
Name : Wildan Panji Tresna
Chief Advisor : Assoc. Prof. Takeo Maruyama
Date of Submission : January, 2020

ABSTRACT

The optical waveguide is one of the good supporting elements in the integrated circuits, because optical waveguide has brought advantages in terms of efficiency, energy consumption and size of the devices. The development of technology in the optical waveguide can be explored for many applications and purposes. Two of the most common types of optical waveguide are channel waveguide and optical slab waveguide. The quality factors of an optical waveguide are usually measured as propagation loss and scattering loss in the optical waveguide.

The silicon-based optical slab waveguide has been intensively studied at 1550 nm wavelength of light. The optical slab waveguide designed in our laboratory is built of silicon as a core, SiO_2 as the bottom layer (substrate) and air as the top cladding layer respectively. In this case, the incident light will be confined and guided in silicon core region. Based on total internal reflection (TIR), we positioned a mirror at 45 degrees from horizontal parallel to light propagation. Furthermore, the effects of the mirror size, curvature radius, length of the slab waveguide and optimization of the coupling system are studied. The loss due to several components such as roughness and imperfectness of the design was comprehensively analyzed. The effect of the mode propagation to the losses are also reviewed. According to

the experimental data on the TE mode propagation, the mirror loss on our slab waveguide is 0.011 dB/mirror and the calculation on the TM mode is 0.007 dB/mirror. The mirror loss can indicate that there has been a slight loss on the mirror which might have been caused by the imperfection of the design of a slab waveguide.

ACKNOWLEDGMENTS

I would like to acknowledge my heartfelt gratitude to *Assoc. Prof. Takeo Maruyama,* for affording me the opportunity to pursue my education through join at High-Speed Laboratory (HS-Lab) as a doctor degree student. During the course, he always kindly supported and gave me invaluable advice on this research that made research progressing and going in the right direction. He also advises me not only the research but also mental attitude as a researcher, deeply analysis and some skill such us presentation technique, and so on. What make confident in my life.

Here, I would also like to thank all of students Lab member *Motoharu Tanizawa, Hiroya Mitsuno, Takuma Ichikawa, Hirotaka Kato, Seiji Kamishima, Tetsuya Yoshida, Masato Shimada, Masataka Tsutsumi* for your togetherness during my course especially for *Alexander William Setiawan Putra* who has been a good partner during course. Also thank you very much for intership student *Nut* and *Mai* from Thailand, *Sun Bohan*, *Gao* and *Lu Shicheng* from China.

Special thanks to Ministry of Research, Technology and Higher Education of the Republic of Indonesia from the RisetPro scholarship which has given the funding for me to continue my research in doctoral course program at Kanazawa University.

Finally, I wish to particularly thank my beloved family for supporting and give me comfort. *Arista* and my beloved children *Zyva*, *Zuhayr* and *Zabyer* for their eternal patience and love. I am grateful to my parents, my young brother, for their continuing support and encouraging me always try to take the giant steps in life.

List of figures

TABLE OF CONTENTS

Chapter 1

Introduction

Current and future technological developments will be greatly influenced by the progress of integrated circuits, both in the electronic, optical or a combination of both. One thing that is very supportive in the development of integrated circuits is the optical waveguide, this is because the optical waveguide has brought increased efficiency, energy consumption and size of the device. The comparison between the development of circuits functionality and the cost per circuit becomes an interesting issue to discuss

Currently the development of optical waveguide can be enjoyed in a variety of applications and purposes, ranging from displays, storage to the field of security. The two most prominent things about the types of optical waveguide that are widely used are channel waveguide and slab or planar waveguide. The quality of an optical waveguide is usually determined by propagation loss and scattering loss. But because the optical waveguide will be connected to an emitter device such as a laser

or LED, there is usually loss due to connectivity, usually called coupling loss. As we all know that the waveguide channel has an advantage in confinement factor but the slab waveguide has other characteristics such as interference and scattering when two propagation lights do not intersect.

A planar waveguide allows light guiding through its volume without significant changes on its properties, thus opening the door to many high technology applications which include the communications, sensors, lasers and optics industrial sectors, among many others. Moreover, a number of new devices may be developed based on optical interconnects to implement distribution systems in parallel or cross-optical signals. The possibility of fabricating planar waveguides using inexpensive and simple technology opens a very interesting field of science.

In the optical slab waveguide, some references have discussed about how to focus light propagation into a waveguide slab, which is by utilizing a fine trapezoidal design which is commonly called a taper.[6-9)] The tapered design also can be applied in many applications in waveguides.[10-13)] Beside the tapered design, other application of slab waveguide that needs to be further developed is the mirror design in slab waveguide. A mirror is usually constructed from differences of the refractive index between the optical waveguide and mirror edge.

The silicon-based optical slab waveguide has been intensively studied at 1550 nm wavelength of light. The optical slab waveguide designed in our laboratory is built of silicon as a core, SiO_2 as the bottom layer (substrate) and air as the top cladding layer respectively. In this case, the incident light will be confined and guided in silicon core region.[23-32)] Based on the refractive index differences between the core, substrate and upper cladding, the mirror in the optical slab waveguide with a 45-degree angle is fabricated and analyzed the mirror loss.[33-36)]

However, inputting the light from the optical fiber into optical slab waveguide is difficult. It is also difficult to collimate this input light during propagation in slab waveguide. To solve these problems, the light propagation is introduced to the slab waveguide through additional taper waveguide to collimate the input light.

In this article, we propose to analyze some optical properties such us propagation loss, coupling loss and the mirror loss for the transverse electric (TE) and transverse magnetic (TM) modes. The characteristic of TE and TM modes when the light source propagates to the waveguide will determine the quality of the waveguides.

1.1. Objective

The main objective of this research is to design, construct, and test by simulation for optical silicon slab waveguide. The design of the slab waveguide consists of the taper design, curve mirror design, half-mirror design and retro reflector design. however, the optical integration in slab waveguide has never been analyzed in detail. The purpose of this research is to measure and analyze in detail about an optical slab waveguide in terms of propagation loss and loss of mirrors. The waveguides must be characterized to know their guiding properties. Furthermore, we also carry out simulations with the FDTD solution in the same design and compare the simulation with experimental results.

1.2. Thesis Organization

In this chapter for introduction, a historical review of the optical technology and developments is discussed at first. And then, as the background of this study, some kind of the optical waveguide such as channel and slab waveguide were argued for completing the application of the optical waveguide.

In the chapter 2, many design of the slab waveguide was realized. The design included the taper, curve mirror, half-mirror design and retro-reflector design. All

of design was described completely, how to get the dimension of the design, hypothesis of the function on each design and also integrated two or three kind of the design on the slab waveguide.

In chapter 3, the characteristic of the slab waveguide was gotten by experiment. The characteristic of the slab waveguide consists of the coupling loss, the waveguide loss and the mirror loss. *Tunable Semiconductor Laser* (TSL) used as a light source with the wavelength 1550 nm and 1mW as an output power. The experimental set up consists of the TSL, single mode fiber, then connected to the rotate wave plate. In the rotate wave plate there are Quarter Wave Plate (QWP) and Half Wave Plate (HWP), the combination between QWP and HWP produce one polarization, that is only TE or TM mode. The polarizing maintenance fiber (PMF) used to keep the output mode from the rotate wave plate, and then connected to the lens fiber to insert the power as much as possible.

In chapter 4, the experimental data and analysis of the propagation loss is reported. In addition, we discuss the influenced of the waveguide length to the propagation loss, also the influenced of the distance between mirrors and the number of mirror to the mirror loss. The coupling loss is very influenced by the size of the optical fiber in the input and output port.

In chapter 5, there will be brief summary of this study and give some future works on this study.

Chapter 2

Silicon waveguide

2.1. Integrated Optics

The term “integrated photonics” refers to the fabrication and integration of several photonic components on a common planar substrate. These components include beam splitters, gratings, couplers, polarizers, interferometers, sources and detectors, among others.

The science that studies the light is called optics. It describes and studies the generation, as well as, the propagation of the light and its interaction with the matter. Optics is an old science, but in the last century it has suffered a spectacular renaissance. The first and more important development in modern optics, without any doubt, was the invention of the laser by T.H. Maiman in 1960 [52]. The development of semiconductor optical devices and the introduction of new fabrication techniques for obtaining optical fibers with very low propagation losses have been important. As a result of these new developments and associated with

other technologies, such as electronics, new disciplines such as electro-optics, opto-electronics, etc. have been generated.

Due to the combination of electronics and optics, new devices, more complex than lasers, semiconductor detectors, light modulators, etc. have appeared. Then a new scientific discipline has arisen to explain these new devices, which are not completely described for optics neither electronics. This scientific branch of applied physics is called photonics. If electronics can be considered as the discipline that describes the flow of electrons, the term of photonics deals with the control of photons.

In integrated photonics, the basic optical elements for generation, focusing, splitting, junction, etc. of light should be integrated in a single optical chip. Thus, the main goal purposed by integrated photonics is therefore the miniaturization of optical systems. This is possible thanks to the small wavelength of the light, which permits the fabrication of circuits and compact photonic devices with sizes of the order of microns.

The integration of passive and active optical devices, in a multicomponent circuit is known as an integrated optic circuit (IOC). Integrated optic devices interface

efficiently with optical fibers, and can reduce the cost in complex circuits by eliminating the need for separate, individual packaging of each circuit element. They also offer smaller size and weight, lower power consumption, improved reliability, and often larger electrical modulation bandwidth compared to their bulk-optic counterparts.

2.2. Introduction to wave guiding

The basic elements of silicon electronics are transistors and interconnects: the transistors perform logic operations, while the interconnects transfer digital information between these transistors. The performance of transistors has steadily been improved by the shrinking of their dimensions. Interconnect performance, however, does not typically get better when sizes are reduced. Electrical interconnects were improved in the past by changing the technology used to fabricate the wiring layers. The ultimate limitations of electrical interconnects have physical, not technological, origins, and these limits are rapidly approaching.

The use of optical links can be the way to avoid the problems of electrical transmission. These optical interconnects are still the most promising candidate to solve the challenges imposed by electrical wiring, both for off-chip and possibly

on-chip applications. [7] The band gap of silicon (~1.1 eV) is such that the material is transparent to wavelengths commonly used for optical transport (around 1.3–1.6μm). One can use standard CMOS processing techniques to sculpt optical waveguides onto the silicon surface. Similar to an optical fiber, these optical waveguides can be used to confine and direct light as it passes through the silicon. [9]

Due to the wavelengths typically used for optical transmission and silicon's high index of refraction, the feature sizes needed for processing these silicon waveguides are on the order of 0.5 – 1 μm. SOI single-mode rib waveguides with core dimensions comparable with single-mode optical fibers have previously been demonstrated. In many cases, these large dimensions are needed because one uses waveguides with a low refractive index contrast. By increasing this index contrast, the confinement can be improved, but this also means that the waveguide core should be reduced in size to keep the waveguide single mode. Then, however, the geometrical features not only become very small but have to be very accurately fabricated. [10]

2.3. Propagation in Theory

A very simple approach to describe the propagation of guided waves in a given medium is the optical ray model, which provides a good understanding of this propagation without having to handle with the solution to Maxwell's equations. [9].

The basic law that this model uses to describe the behavior of propagating waves in the surface between two mediums (or interface) with different refractive indexes is Snell's Law, which says that an incident field to this surface will be partly transmitted and partly reflected.:

$$n_1 \sin\theta_1 = n_2 \sin\theta_2 \tag{2.1}$$

being n_1 and n_2 the refractive indexes of the mediums, and θ_1 and θ_2 the angle of reflection and the angle of transmission, respectively.

It can be demonstrated from this law that angles smaller than a critical angle θc will experiment total internal reflection (TIR), which means that there is no transmitted field. This angle is given by the next expression:

$$\sin\theta_c = \frac{n_2}{n_1} \tag{2.2}$$

This law applies also in the case of generic slab waveguides, like the one depicted in Figure 2.1. It can be shown that the propagation in such a waveguide will experiment total internal reflection in both interfaces.

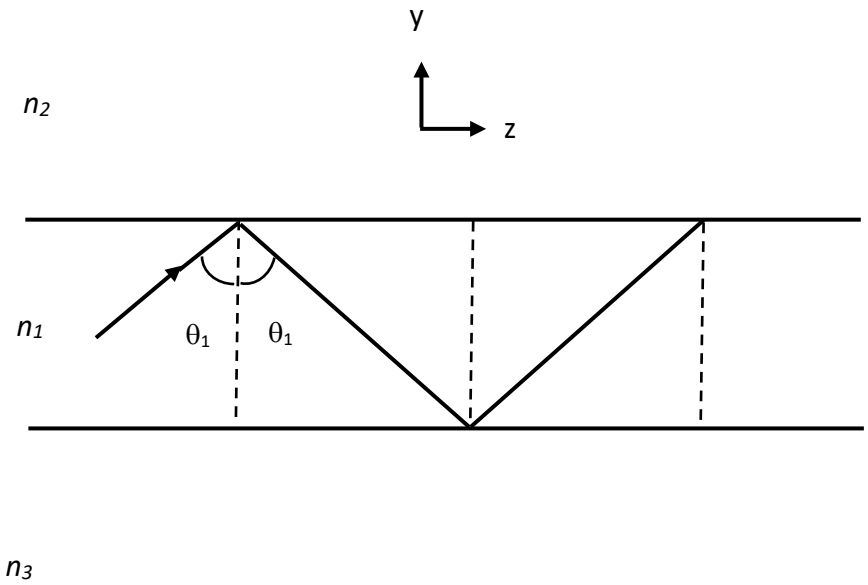

Figure 1. Propagation light on the three layers of the different material

In general, $n_1 > n_2, n_3$ to ensure propagation by total internal reflection. In the case of $n_2 = n_3$ the waveguide is called symmetrical, and asymmetrical if not. In the following sections the basic characteristics of guided waves are described, which will be used to characterize and describe the behavior and performance of optical devices.

2.3.1 Polarization

The fields that can propagate in a medium are normally classified in two possible polarizations: transverse electric (TE), when the electric field is perpendicular to the plane of incidence, or transverse magnetic (TM), when the magnetic field is perpendicular to the same plane. [9] TE and TM modes in an optical waveguide do not have a uniform linear polarization direction, so cannot be described as horizontal or vertical. In TE modes, the electric field vector is everywhere transverse and perpendicular to the waveguide axis. In TM modes, the magnetic field is the transverse. In a circular dielectric waveguide such as an optical waveguide, the electric field of the TM modes is largely radial with a small axial component, and the transverse magnetic field is circumferential. For TE modes, the magnetic field is radial, and the electric field direction circular. In both TE and TM modes, the transverse field components are zero at the center of the optical waveguide.

2.3.2 Mode in waveguide

However, light only propagates in a set of allowed discrete angles. The equation that has to be solved (for TE modes) in a generic asymmetrical waveguide is the following:

$$k_0 n_1 h \cos\theta_1 - m\pi = \tan^{-1}\sqrt{\frac{\sin^2\theta_1 - \left(\frac{n_2}{n_1}\right)^2}{\cos\theta_1}} + \tan^{-1}\sqrt{\frac{\sin^2\theta_1 - \left(\frac{n_3}{n_1}\right)^2}{\cos\theta_1}} \qquad 2.3$$

with $k = \frac{2\pi}{\lambda}$ the propagation constant in free space and h the height of the core layer. Every allowed angle gives place to a specific field, also called mode of propagation, and is indicated by its mode number with the index m. The mode with $m = 0$ is known as fundamental mode. For every interface the critical angle will be different, so the angle that guarantees total internal reflection in both interfaces is the one that gives solution to this equation (the larger). Single mode conditions can be derived from this equation. Single mode waveguides do not suffer from intermodal dispersion, which is the dispersion caused by the different velocities with which every mode travels in the waveguide. In this way the shape of the transmitted signal remains more similar after going through the waveguide. In addition, if the waveguide is multimode, the total power transmitted has to be shared by all the modes, and so the fundamental mode has lower power**.**

2.4. Optical Waveguide

An optical waveguide is a basic waveguide for configuring an optical integrated circuit, a semiconductor laser, or the like, and generally has a structure in which a core having a square or rectangular cross section is surrounded by a clad having a lower refractive index. An example of the structure of an optical waveguide is shown in Fig. 2. In the Figure 2 (a) shows a slab optical waveguide, in this case, light is confined only in the *x* direction and propagates in the *z* direction. In contrast, in the channel optical waveguide shown in Fig. 2 (b), light is confined in the *x* and *y* directions and propagates in the *z*-direction.

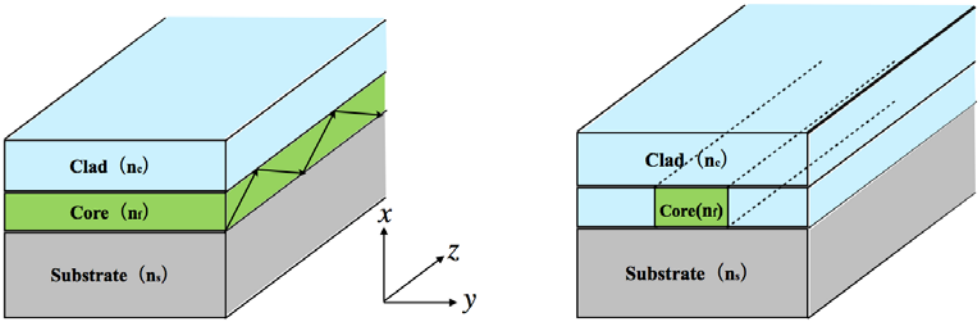

Figure 2. The slab waveguide and channel waveguide on the side view

2.5. Maxwell Equation

Since light is an electromagnetic wave, it follows Maxwell's equation. Maxwell's equations describe how electric and magnetic fields are generated by charges, currents, and changes of the fields. An important consequence of the equations is that they demonstrate how fluctuating electric and magnetic fields propagate at a constant speed (*c*) in a vacuum. In the waveguide Maxwell's equations are shown below.

$$div\ D\ = \rho \tag{2.4}$$

$$div\ B\ = 0 \tag{2.5}$$

$$rot\ E\ = -\frac{\partial B}{\partial t} \tag{2.6}$$

$$rot\ H\ = J\ + \frac{\partial D}{\partial t} \tag{2.7}$$

Where *E* is the electric field, *D* is the electric flux density, *H* is the magnetic field, *B* is the magnetic flux density, ρ is the charge density, and *J* is the current density. In general, the electric flux density *D*, magnetic flux density *B*, and current density *J* can be expressed by the following equations.

$$D = \varepsilon E = \varepsilon_0 \varepsilon_S E \quad (2.8)$$

$$B = \mu H = \mu_0 \mu_S H \quad (2.9)$$

$$J = \sigma E \quad (2.10)$$

Where ε is the dielectric constant of the medium, μ is the magnetic permeability of the medium, ε_s is the relative dielectric constant of the medium, μ_r is the relative magnetic permeability of the medium, σ is the conductivity, ε_0 is the dielectric constant in vacuum, and μ_0 is in the vacuum Is the magnetic permeability. About light waves

$$\mu_r = 1, \qquad J = 0, \qquad \rho = 0, \qquad \sigma = 0$$

Are often considered, and Maxwell's equations are given below.

$$rot\ E = -\mu_0 \frac{\partial H}{\partial t} \quad (2.11)$$

$$rot\ H = \varepsilon \frac{\partial E}{\partial t} \quad (2.12)$$

Consider the propagation of a plane wave expressed by the following equation.

$$E = E_{(x,y)} e^{j(\omega t - \beta z)} \tag{2.13}$$

$$H = H_{(x,y)} e^{j(\omega t - \beta z)} \tag{2.14}$$

Here, β is a propagation constant, and ω is the angular frequency of light. Substituting the above equation into Maxwell's equations (2.11) and (2.12).

$$rot\ E = -\mu_0 \frac{\partial}{\partial t}\{H_{(x,y)} e^{j(\omega t - \beta z)}\} = -j\omega\mu_0 H \tag{2.15}$$

$$rot\ H = \varepsilon \frac{\partial}{\partial t}\{E_{(x,y)} e^{j(\omega t - \beta z)}\} = j\omega\varepsilon E \tag{2.16}$$

When said formula is divided into each component, it is expressed by the following formula.

$$\frac{\partial E_z}{\partial y} - \frac{\partial E_y}{\partial z} = -j\omega\mu_0 H_x \tag{2.17}$$

$$\frac{\partial E_x}{\partial z} - \frac{\partial E_z}{\partial x} = -j\omega\mu_0 H_y \tag{2.18}$$

$$\frac{\partial E_y}{\partial x} - \frac{\partial E_x}{\partial y} = -j\omega\mu_0 H_z \tag{2.19}$$

$$\frac{\partial H_z}{\partial y} - \frac{\partial H_y}{\partial z} = j\omega\varepsilon E_x \tag{2.20}$$

$$\frac{\partial H_x}{\partial z} - \frac{\partial H_z}{\partial x} = j\omega\varepsilon E_y \qquad (2.21)$$

$$\frac{\partial H_y}{\partial x} - \frac{\partial H_x}{\partial y} = j\omega\varepsilon E_z \qquad (2.22)$$

Consider a plane wave (one-dimensional wave) propagating in a homogeneous medium in the z direction. For plane waves, E and H are constant in any *xy*-plane, so $\frac{\partial}{\partial_x} = 0$ and $\frac{\partial}{\partial_y} = 0$. Therefore, the plane waves propagating in the *z* direction from Eq. (2.19) and (2.22) are $H_z = 0$ and $E_z = 0$, and have no component in the propagation direction. It can also be divided into two equations: equations containing only E_x and H_y (Equations (2.18) and (2.20)) and equations containing only H_x and E_y (Equations (2.17) and (2.21)). This solves the equations for H_x and E_y. Partially differentiate equation (2.17) by z.

$$\frac{\partial^2 E_y}{\partial x^2} = j\omega\mu_0 \frac{\partial H_x}{\partial z} \qquad (2.23)$$

Substitute equation (2.21) into equation (2.23).

$$\frac{\partial^2 E_y}{\partial x^2} = j\omega\mu_0 \times j\omega\varepsilon E_y = -\omega^2\varepsilon\mu_0 E_y \qquad (2.24)$$

The solution of this wave equation is expressed by the following equation.

$$E_y = Ae^{-i\omega\sqrt{\varepsilon\mu_0}\,z} + Be^{i\omega\sqrt{\varepsilon\mu_0}\,z} \quad (2.25)$$

The first term on the right side represents a wave traveling in the positive z-direction, and the second term represents a wave traveling in the negative z-direction.

Consider the case in a vacuum. Since $\varepsilon = \varepsilon_0$ in a vacuum, $\omega\sqrt{(\varepsilon\mu_0)}$ becomes $\omega\sqrt{(\varepsilon_0\mu_0)}$. The portion of $\omega\sqrt{(\varepsilon_0\mu_0)}$ represents the phase rotation angle when moving 1 m in the z- direction, which is called wave number in vacuum, and is represented by k_0.

$$k_0 = \omega\sqrt{\varepsilon_0\mu_0} \quad (2.26)$$

Further, the wavelength in vacuum is represented by λ, and since it rotates 2π at one wavelength, the rotation angle per 1 m is represented by the following formula.

$$k_0 = \frac{2\pi}{\lambda} \quad (2.27)$$

The following equation is obtained from equations (2.26) and (2.27).

$$\frac{1}{\sqrt{\varepsilon_0\mu_0}} = f\lambda = c \quad (2.28)$$

When c is the speed of light in vacuum, and $c = 3 \times 10^8$ m⁄s.

Next, consider the case of propagating through a medium with a refractive index of n. From the relationship of $\varepsilon = \varepsilon_S \varepsilon_0$ and $\varepsilon_S = n^2$, $\omega \sqrt{(\varepsilon\mu_0)} = \omega \sqrt{(\varepsilon_0\mu_0)}$ $n = k_0 n$. Thus, the wave number of the plane wave propagating through the medium having the refractive index n is $k_0 n$. Therefore, the speed of light is $\frac{1}{n}$ in a medium having a refractive index n.

2.6 Boundary Condition

Consider a situation where two different media with ε_1, ε_2 and permeability μ_1, μ_2 are in contact. When the tangential component is placed on the boundary surface of the electromagnetic field in each medium as E_{t1}, E_{t2}, H_{t1}, H_{t2}, and the normal component is placed on the boundary surface as E_{n1}, E_{n2}, H_{n1}, H_{n2}, the electromagnetic field satisfies the following conditions.

$$\begin{cases} E_{t1} = E_{t2} \\ H_{t1} = H_{t2} \end{cases} \tag{2.29}$$

$$\begin{cases} \varepsilon_1 E_{n1} = \varepsilon_2 E_{n2} \\ \mu_1 H_{n1} = \mu_1 H_{n2} \end{cases} \tag{2.30}$$

That is the tangential components of the electric field and the magnetic field are continuous at the boundary surface of the medium, and the normal components of the electric flux density and the magnetic flux density are also continuous.

2.7 Optical Power

The pointing vector *S* representing the energy density of the electromagnetic field is defined by the following equation.

$$S_{(t)} = E_{(t)} \times H_{(t)} \tag{2.31}$$

Equation (2.31) is the instantaneous value of the light energy flux. The effective value (time average) of the pointing vector is also called irradiance. When the electromagnetic wave is a single frequency standing wave, the value is expressed by the following equation.

$$S = Re\left[\frac{E \times H^*}{2}\right] \tag{2.32}$$

Here, * represents a complex conjugate. The optical power passing through a certain surface is obtained by the area of the pointing vector.

2.8 Optical Slab Waveguide

In order to analyze the propagation characteristics of light waves in an optical waveguide, a three-dimensional analysis is required. An actual optical waveguide device is also composed of a three-dimensional channel optical waveguide. However, computer analysis is often necessary for rigorous analysis in three dimensions, and results are not always good. Therefore, first, a flat (two-dimensional) slab optical waveguide is taken up and a wave optical analysis is performed.

2.8.1 Wave equations in optical slab waveguides

When considering a slab optical waveguide, $\frac{\partial}{\partial_y} = 0$ because there is no dependence of the electromagnetic field on the *y*-axis as shown in Fig. 2 (a). To simplify the analysis, analysis is divided into TE mode (H_x, E_y, H_z) where the principal component of the electric field is the x component and TM mode (E_x, H_y, E_z) where the principal component of the electric field is the y component. Is often used. After that, the wave equation, which is the basic equation, is derived by dividing into TE mode and TM mode. Also, $\frac{\partial}{\partial_z}$ = -j β.

2.8.1.1 TE Mode

In the TE mode, the electric field is polarized in the x direction, so that $E_x = H_y = E_z = 0$. Therefore, equations (2.17) to (2.22) are represented by the following equations.

$$H_x = -\frac{\beta}{\omega\mu_0} E_y \tag{2.33}$$

$$H_z = -\frac{1}{j\omega\mu_0} \frac{\partial E_y}{\partial x} \tag{2.34}$$

$$\frac{\partial^2 E_y}{\partial x^2} + (k_0 n^2 - \beta^2) E_y = 0 \tag{2.35}$$

2.8.1.2 TM mode

In the TM mode, since the electric field is polarized in the x direction, $H_x = E_y = H_z = 0$. Therefore, equations (2.17) to (2.22) are represented by the following equations.

$$E_x = \frac{\beta}{\omega\varepsilon_0 n^2} H_y \tag{2.36}$$

$$E_z = \frac{1}{j\omega\varepsilon_0 n^2} \frac{\partial H_y}{\partial x} \tag{2.37}$$

$$n^2 \frac{d}{dx}\left(\frac{1}{n^2}\frac{dH_y}{dx}\right) + (k_0 n^2 - \beta^2) H_y = 0 \tag{2.38}$$

2.8.2 Dispersion Equation

Consider the case where the electromagnetic field component ϕ *(x, z)* of the light wave propagating in the slab waveguide is separated as follows.

$$\phi(x,z) = \phi(x)e^{j\beta z} \tag{2.39}$$

Here, β is called a propagation constant and represents the wave number of the light wave propagating in the waveguide. Also, where $\beta = k0N$ is called the equivalent refractive index or effective refractive index. The equivalent refractive index satisfies the following condition.

$$max\{n_C, n_S\} < N < n_f \tag{2.40}$$

Here, an equation representing the dispersion relation of the slab waveguide for each of the TE mode and the TM mode, that is, a dispersion equation is derived.

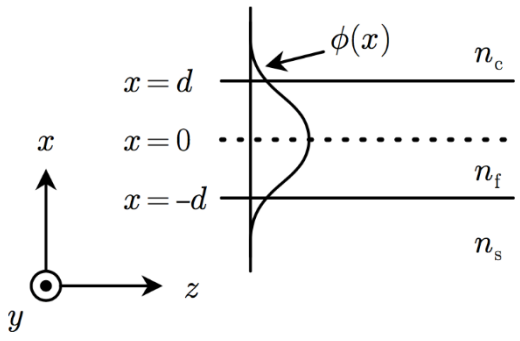

Figure 3. Beam profile on the three layers of the different material

2.8.2.1 TE Mode

Consider the case where the electric field E_y (x, z) is separated as follows.

$$E_y(x,z) = E_y(x)e^{j\beta z} \tag{2.41}$$

In the optical waveguide, the light wave is confined in the core and the nearby region, so $E_y = 0$ at infinity (x = ± ∞). At this time, the general solution of equation (2.35) is expressed by the following equation.

$$E_y = Ae^{j\left(\sqrt{k_0 n^2 - \beta^2}\right)z} + Be^{-j\left(\sqrt{k_0 n^2 - \beta^2}\right)z} \tag{2.42}$$

When the solution that does not diverge at (x = ± ∞) is selected and the electromagnetic field distribution in each region is obtained, it is expressed by the following equation.

$$E_y(x) = \begin{cases} E_C e^{-\sigma(x-d)} & (x > d) \\ E_f \cos(\kappa x - \phi) & (-d \le x \le d) \\ E_S e^{\xi(x+d)} & (x < -d) \end{cases} \tag{2.43}$$

Here, σ, κ, ξ are represented by the following equations.

$$\begin{cases} \sigma = \sqrt{\beta^2 - k_0^2 n_C^2} = k_0 \sqrt{N^2 - n_C^2} \\ \kappa = \sqrt{k_0^2 n_f^2 - \beta^2} = k_0 \sqrt{n_f^2 - N^2} \\ \xi = \sqrt{\beta^2 - k_0^2 n_S^2} = k_0 \sqrt{N^2 - n_S^2} \end{cases} \tag{2.44}$$

Here, since the electromagnetic field is continuous at the boundary of the medium different from the boundary condition expression (2.29), the following boundary condition is satisfied.

$$E_C = E_f \cos(\kappa x - \phi) \tag{2.45}$$

$$E_S = E_f \cos(\kappa x + \phi) \tag{2.46}$$

$$\sigma E_C = \kappa E_f \cos(\kappa x - \phi) \tag{2.47}$$

$$\xi E_S = \kappa E_f \cos(\kappa x + \phi) \tag{2.48}$$

From equations (2.42), (2.44) to (2.47), the following equation is obtained.

$$E_y(x) = \begin{cases} E_f \cos(\kappa x - \phi)\, e^{-\sigma(x-d)} & (x > d) \\ E_f \cos(\kappa x - \phi) & (-d \le x \le d) \\ E_f \cos(\kappa x + \phi)\, e^{\xi(x+d)} & (x < -d) \end{cases} \tag{2.49}$$

$$tan(\kappa x - \phi) = \frac{\sigma}{\kappa} \tag{2.50}$$

$$tan(\kappa x - \phi) = \frac{\xi}{\kappa} \tag{2.51}$$

Further, the following equations are obtained from the equations (2.49) and (2.50).

$$\kappa d = \frac{m\pi}{2} + \frac{1}{2} tan^{-1}\left(\frac{\xi}{\kappa}\right) + \frac{1}{2} tan^{-1}\left(\frac{\sigma}{\kappa}\right) \tag{2.52}$$

$$\phi = \frac{m\pi}{2} + \frac{1}{2} tan^{-1}\left(\frac{\xi}{\kappa}\right) - \frac{1}{2} tan^{-1}\left(\frac{\sigma}{\kappa}\right) \tag{2.53}$$

$(m = 0, 1, 2, 3, \cdots)$

Here, ầnd m are parameters called mode numbers, and the guided mode corresponding to a certain m is called the m-th mode. Equation (2.41) is the dispersion equation in the TE mode. The propagation constant β can be determined by giving the structure (n_c, n_f, n_s, d), wavelength λ, and mode number m of the optical waveguide.

Next, standardize the dispersion equation and modify it so that it can be applied to any slab waveguide. The normalized frequency *V*, normalized propagation constant b, and waveguide asymmetry measure a are defined as follows.

$$V = k_0 d\sqrt{n_f^2 - n_S^2} = \frac{\omega d}{c}\sqrt{n_f^2 - n_S^2} \tag{2.54}$$

$$b = \frac{N^2 - n_S^2}{n_f^2 - n_S^2} \tag{2.55}$$

$$a = \frac{n_S^2 - n_C^2}{n_f^2 - n_S^2} \tag{2.56}$$

By transforming equation (2.51) using equations (2.53) to (2.55), the following standardized dispersion equation is obtained.

$$2V\sqrt{1-b} = m\pi + tan^{-1}\sqrt{\frac{b}{1-b}} + tan^{-1}\sqrt{\frac{a+b}{1-b}} \tag{2.57}$$

Fig. 4 shows the *b*-*V* curve obtained from equation (2.56). From Figure 4 the zero-order mode exists for every *V* when a = 0, that is, when $n_S = n_C$. That is, at least one waveguide mode exists in a slab waveguide having a symmetric refractive index distribution. On the other hand, the other modes do not exist in the region below a certain *V*. Such a state is called a cutoff.

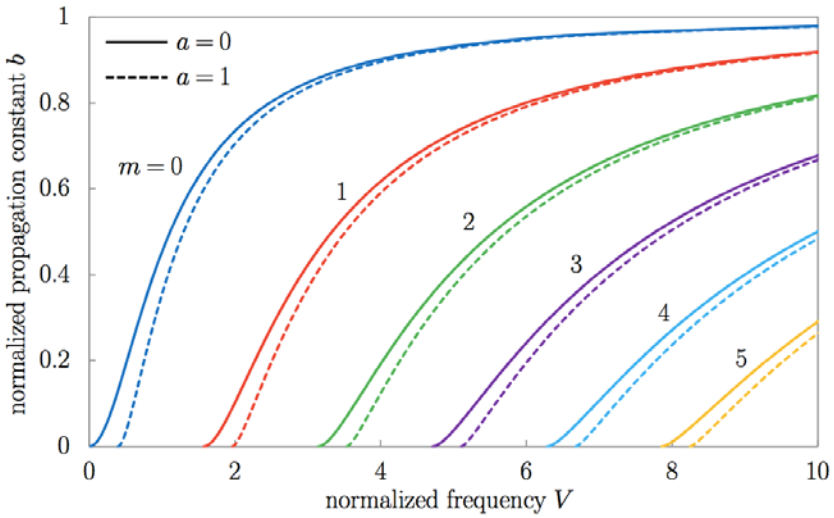

Figure 4. Normalized propagation constant dependence of the normalize frequency on TE and TM mode.

2.8.2.2 TM Mode

As in the case of the TE mode, the solution of equation (2.38) yields the following equation.

$$H_y(x) = \begin{cases} H_c e^{-\sigma(x-d)} & (x > d) \\ H_f \cos(\kappa x - \phi) & (-d \le x \le d) \\ H e^{\xi(x+d)} & (x < -d) \end{cases} \tag{2.58}$$

Here, σ, κ, ξ are represented by the following equations.

$$\begin{cases} \sigma = \sqrt{\beta^2 - k_0^2 n_C^2} = k_0\sqrt{N^2 - n_C^2} \\ \kappa = \sqrt{k_0^2 n_f^2 - \beta^2} = k_0\sqrt{n_f^2 - N^2} \\ \xi = \sqrt{\beta^2 - k_0^2 n_S^2} = k_0\sqrt{N^2 - n_S^2} \end{cases} \tag{2.59}$$

Although the electromagnetic field is continuous at the boundary between different media, since $\frac{1}{\mathrm{n}^2}\frac{\partial_{Hy}}{\partial_x}$ is continuous instead of H_y from equation (2.37), the following equation is obtained.

$$H_C = H_f\, cos(\kappa x - \phi) \tag{2.60}$$

$$H_S = H_f\, cos(\kappa x + \phi) \tag{2.61}$$

$$\sigma n_C^2 E_C = \kappa n_f^2 H_f\, cos(\kappa x - \phi) \tag{2.62}$$

$$\xi n_S^2 E_S = \kappa n_f^2 H_f\, cos(\kappa x + \phi) \tag{2.63}$$

The following equations are obtained from Equations (2.57) to (2.62).

$$H_y(x) = \begin{cases} H_f\, cos(\kappa x - \phi)\, e^{-\sigma(x-d)} & (x > d) \\ H_f\, cos(\kappa x - \phi) & (-d \le x \le d) \\ H_f\, cos(\kappa x + \phi)\, e^{\xi(x+d)} & (x < -d) \end{cases} \tag{2.64}$$

$$tan(\kappa x - \phi) = \frac{\sigma n_f^2}{\kappa n_C^2} \tag{2.65}$$

$$tan(\kappa x - \phi) = \frac{\xi n_f^2}{\kappa n_S^2} \tag{2.66}$$

From equations (2.64) and (2.65), a dispersion equation for the TM mode is obtained by the following equation.

$$\kappa d = \frac{m\pi}{2} + \frac{1}{2}\tan^{-1}\left(\frac{\xi n_f^2}{\kappa n_S^2}\right) + \frac{1}{2}\tan^{-1}\left(\frac{\sigma n_f^2}{\kappa n_C^2}\right) \tag{2.67}$$

$$\kappa d = \frac{m\pi}{2} + \frac{1}{2}\tan^{-1}\left(\frac{\xi n_f^2}{\kappa n_S^2}\right) - \frac{1}{2}\tan^{-1}\left(\frac{\sigma n_f^2}{\kappa n_C^2}\right) \tag{2.68}$$

$(m = 0, 1, 2, 3, \cdots)$

Also, as in the case of the TE mode, Expression (3.63) is normalized using Expressions (2.53) to (2.55). The normalized TM mode dispersion equation is shown below.

$$2V = \sqrt{1-b} = m\pi + tan^{-1}\left(\frac{n_f^2}{n_S^2}\sqrt{\frac{b}{1-b}}\right) + tan^{-1}\left(\frac{n_f^2}{n_C^2}\sqrt{\frac{a+b}{1-b}}\right) \tag{2.69}$$

Figure 4 shows dispersion curves of the TE mode and the TM mode when n_f = 3.47, n_S = n_C = 1.44, and a = 0. While the normalized dispersion curve of the

TE mode does not depend on the refractive index of the waveguide material, the rise of the curve becomes gentler as the relative refractive index difference increases in the TM mode.

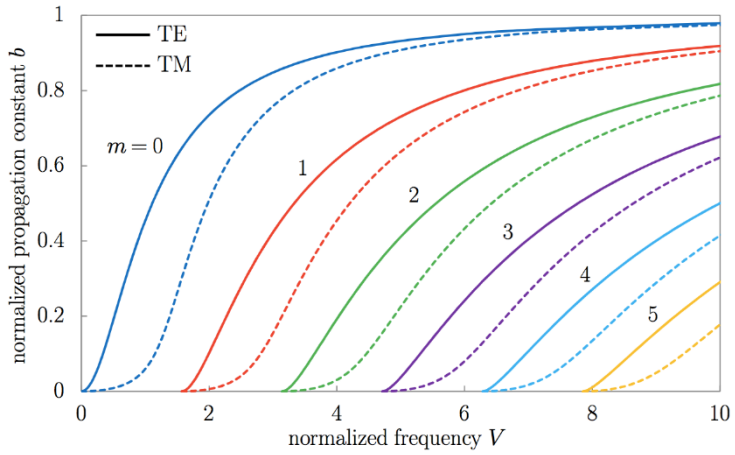

Figure 4. Normalized propagation constant dependence of the normalize frequency on TE and TM mode.

2.9 Finite Different Time Domain

The Finite Difference Time Domain method (FDTD) is a method of discretizing the time-domain analysis formula of Maxwell's equation in space and time, and numerically calculating it as a difference equation. Since no

approximation other than discretization is included, the calculation accuracy is good under sufficiently fine difference width. In addition, since it is a numerical analysis method in the time domain, it is possible to perform a spectrum analysis by one simulation by performing a Fourier transform on the obtained solution. Although it is a method that is easy to implement but requires a large amount of computation, it is now considered to be the mainstream numerical calculation algorithm for electromagnetic field analysis due to recent improvements in computer performance.

In this research, the FDTD method is uses in simulation software to do some calculation, and the software has included all the theoretical calculations. So that, the simulation software helps to develop and analysis deeply in the characteristics of the slab waveguide.

2.10 Gaussian Beam and Beam Divergence

In most applications, the propagation characteristics of laser beam is necessary to be known. In general, laser beam propagation can be assuming that the laser beam has an ideal Gaussian intensity profile that can be expressed as

$$I(r) = I(0)exp\left(-\frac{2r^2}{{\omega_0}^2}\right), \qquad (2.70)$$

where *r* is defined as the distance from the center of the beam, and ω_0 is the radius at which the amplitude is $\frac{1}{e}$ of its value on the axis.

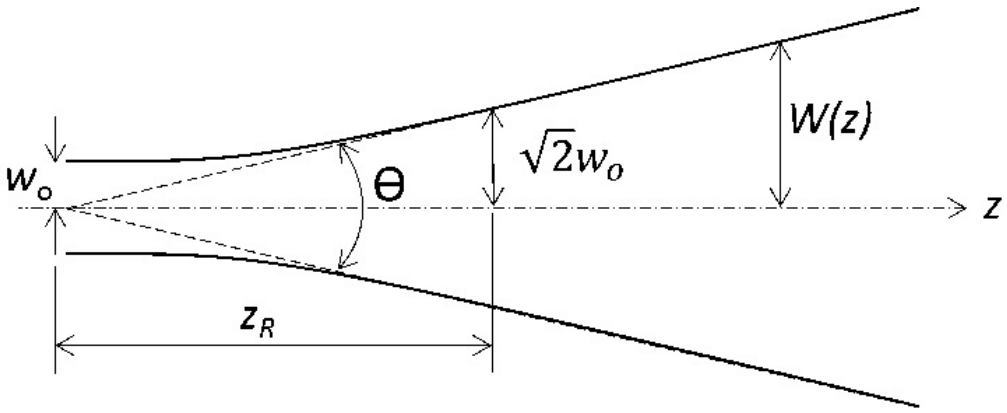

Figure 5. Gaussian beam propagation in free space

From the Fig. 5, a Gaussian beam propagating in free space, the spot size *w(z)* will be at minimum value w_o at a place along the beam axis, known as the beam waist. For a beam of wavelength λ at a distance *z* along the beam from the beam waist, it is also called the edge of a beam radius where *r = w(z)*, the variation of the spot size is given by:

$$w(z) = w_o\sqrt{1 + \left(\frac{z}{z_R}\right)^2}, \qquad (2.71)$$

where the origin of the *z*-axis is defined without loss of generally to coincide with the beam waist, and the Rayleigh distance or Rayleigh range z_R is determined by

$$z_R = \frac{\pi {w_o}^2}{\lambda}. \tag{2.72}$$

Therefore, the condition where $z \gg z_R$ the parameter *w(z)* increases linearly with *z.* It is mean that far from waist, the beam edge is cone-shaped. The angle between lines along that cone and the central axis of the beam is called divergence of the beam, that given by

$$\theta \approx \frac{\lambda_0}{\pi \omega_0 n}, \tag{2.73}$$

where, *n* is the refractive index of the medium the beam propagates through, and λ_0 is the free-space wavelength. When the directivity angle is sufficiently small, the total angular spread of the beam far from the waist, and is given by

$$\Theta \ = 2\theta = 2tan^{-1}\left(\frac{\lambda_0}{\pi \omega_0 n}\right) \approx 2tan^{-1}\left(\frac{D_f - D_i}{2L}\right). \tag{2.74}$$

The divergence of a beam also can be calculated if one knows the beam diameter at two separate points far from any focus D_i and D_f on distance *L* between these points.

2.10.1 Collimated Beam

A collimated beam of light is a beam typically a laser beam, which has a low beam divergence so that the beam radius does not undergo significant changes within reasonable propagation distance. In the case of Gaussian beams, the Rayleigh length must be long compared with the envisaged propagation distance. The Rayleigh length scales with the square of the beam waist radius so that large beam radius is essential for long propagation distances.

A divergent beam can merely be collimated with a lens or a curved mirror, where the focal length or curvature radius is chosen such that the curved initially wave fronts become flat, which can be seen in Figure 6.

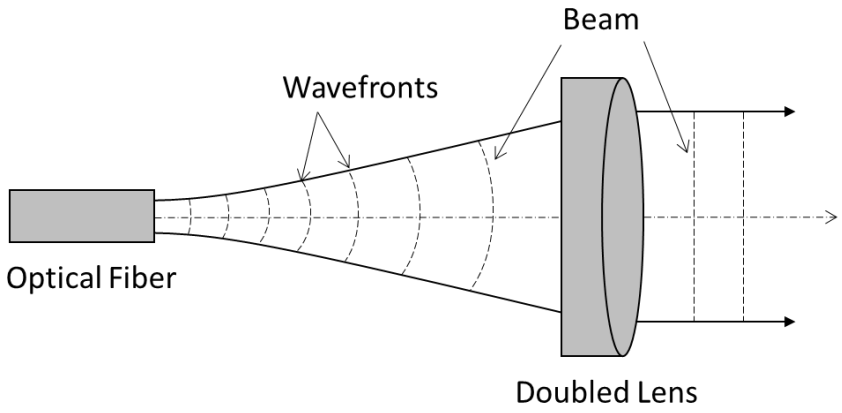

Figure 6. A doubled lens collimates the output beam from a fiber

Collimated beams are very useful to emitting in long distance for several applications like wireless power or data transfer, because the beam radius stays approximately constant, so that the distances between optical components may be readily varied without applying extra optics, and excessive beam radius is avoided. Most solid-state lasers naturally emit collimated beams, a flat output coupler enforces flat wave fronts at the output, and the beam waist is usually large enough to avoid excessive divergence. Edge-emitting laser diodes, however, emit strongly diverging beams and are therefore often equipped with collimation optics, with a collimator, largely reducing the strong divergence.

The analysis about the collimated beam is very useful in discussing about the taper design in slab waveguide. The details of the taper design will be explained in the chapter. 3

Chapter 3

Design and Simulation

3.1 Introduction

The slab waveguide consists of three layers of materials with different dielectric constants, extending infinitely in the directions parallel to their interfaces. The light may be confined in the middle layer by total internal reflection. This occurs only if the dielectric index of the middle layer is larger than that of the surrounding layers. In practice slab waveguides are not infinite in the direction parallel to the interface, but if the typical size of the interfaces is much larger than the depth of the layer, the slab waveguide model will be an excellent approximation.

On the application, the function and characteristics of a slab waveguide are determined by its design. The constructed design by using taper to connect channel waveguide to slab waveguide as shown in Fig. 7

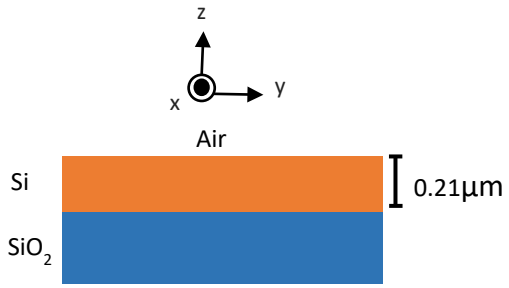

Figure 7. Cross section of a slab waveguide

In its application it is very difficult to guide the light that comes directly inside the slab waveguide, considering the confinement factor in the slab waveguide is only limited to 1-dimension. For this reason, many researchers propose using a grating coupler or spot size converter, meanwhile from the design side to be propagated use taper design.

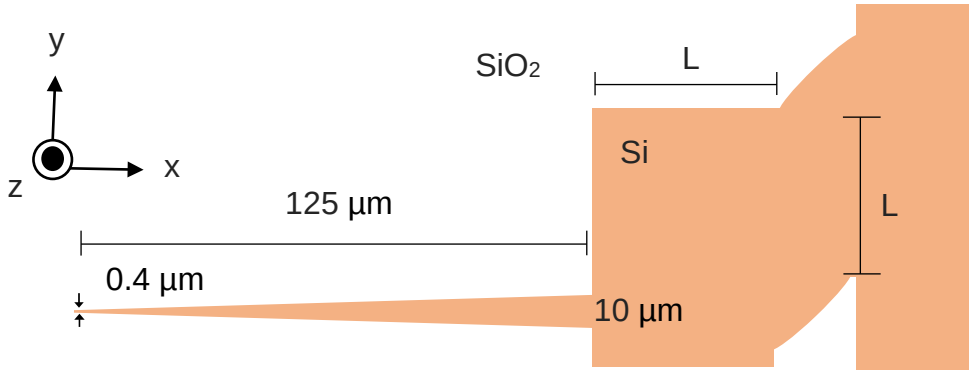

Figure 8. Cross section of a slab waveguide

The slab waveguide which is connected with the channel waveguide, with 0.4 μm in width and 0.21 μm in thickness as shown in Fig. 8. The slab waveguide is constructed by the Si as a core and SiO_2 as the substrate. The taper design with 125 μm in length, 0.4 μm of input port, and 10 μm of output port is designed after the channel to keep the light propagates in parallel. The slab waveguide is constructed of silicon with an effective refractive index (n_{eff}) of 2.83 as a core and SiO_2 with a refractive index of (n) 1.47 as the substrate. The refractive index difference makes the light to propagate to the x-direction inside of the silicon waveguide only.

3.2 Design

3.2.1. Taper design

The function of the taper is to obtain an efficient coupling between two different optical waveguides which are channel waveguide and the slab waveguide. Normally, the function of the taper is to change the size and the shape of the optical propagation. The linear taper is adapted to this design as shown in Fig. 9.

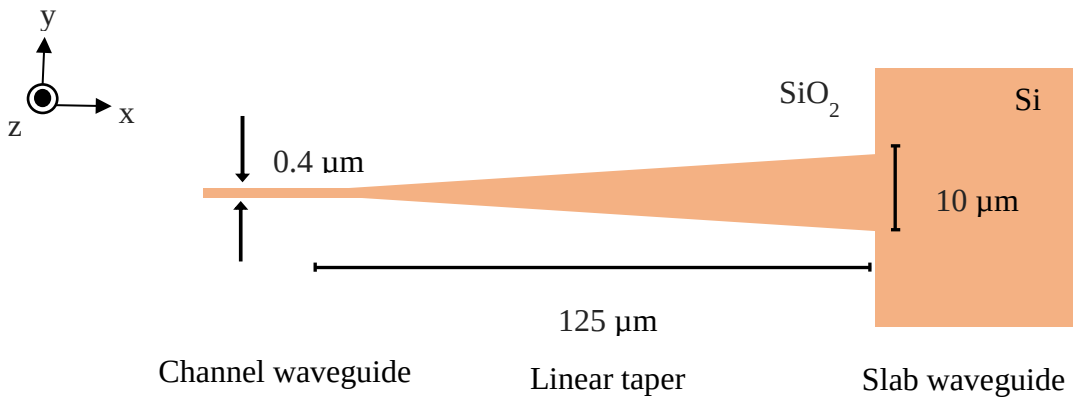

Figure 9. The taper design on the slab waveguide

The taper design with 125 µm in length, 0.4 µm of the input port, and 10 µm of the output port is designed after the channel waveguide to control the divergence angle of the input light of slab waveguide. Using taper structure, the divergence angle of the input light of slab waveguide can be kept small.

The tapered design carries out the parallel pattern of the light with small divergence angle, even though the output beam size is larger than the input as shown in Fig. 10.

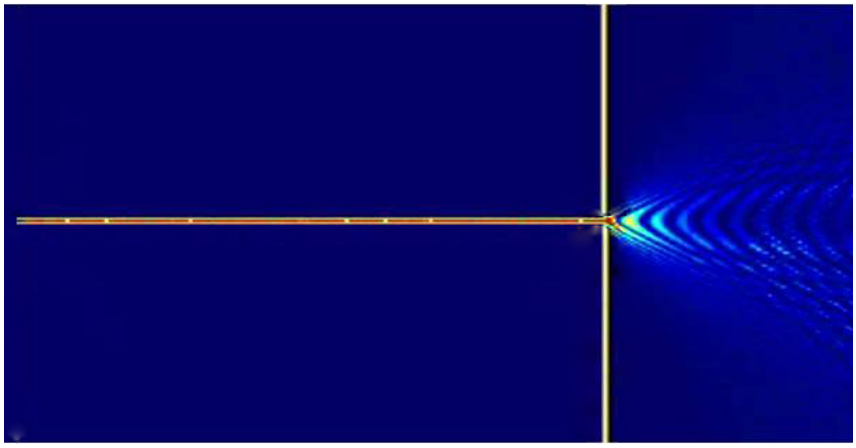

(a)

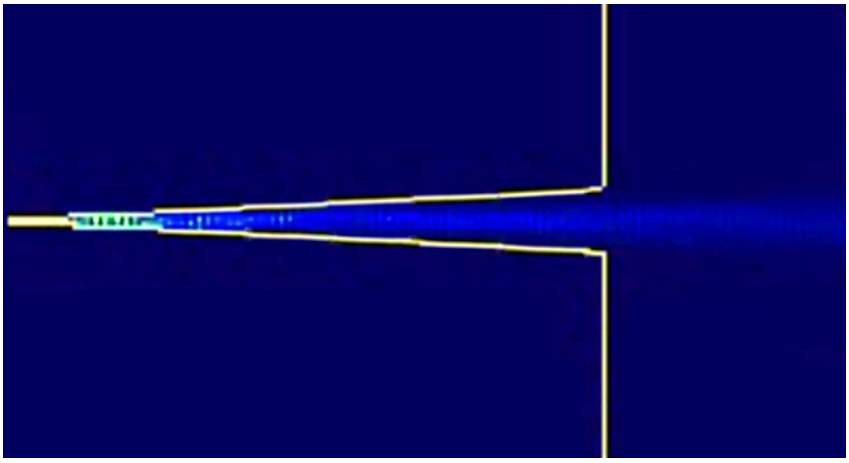

(b)

Figure 10. Simulation result of the slab waveguide without and with the taper design.

The FDTD simulations are used to investigate the effect of the tapered design as shown in Fig. 10. The taper keeps the incident light in parallel conditions so that the optical power can be detected at long distances. In this case the divergence angle of the beam can be kept being small using taper. The taper design causes the optical power of the narrow input to be gradually blocked so that it produces a straight path with a very small divergent angle.

We also want to see the power distribution along the propagation path that is passed, so we do a simulation using a power monitor and place it at the taper output and after a distance of 50 μm from the position of the first power monitor. By installing a power monitor in the two positions, you can compare the condition of the optical spectrum in both positions, so that you can also find out the width of the optical spectrum after a distance of 50 μm. and the width of the optical spectrum can be used to determine how wide the monitor power is needed in a simulation.

Then we make variations in the length of the taper and observe the width of the optical spectrum, in this case the optical spectrum is represented by Full Width Half Maximum (FWHM). in this simulation, variations in taper length are made from a range of 50 μm to 150 μm as shown in Fig. 11 regarding the taper length vs FWHM graph. In the range of taper length between 50 μm to 150 μm it looks like

the uneven step variation, this is because at a distance of 50 µm is the shortest taper length condition, so according to the hypothesis it will not provide maximum optical power. In this simulation the FWHM output width of the taper is 10 µm and the wavelength used in this simulation is 1550nm.

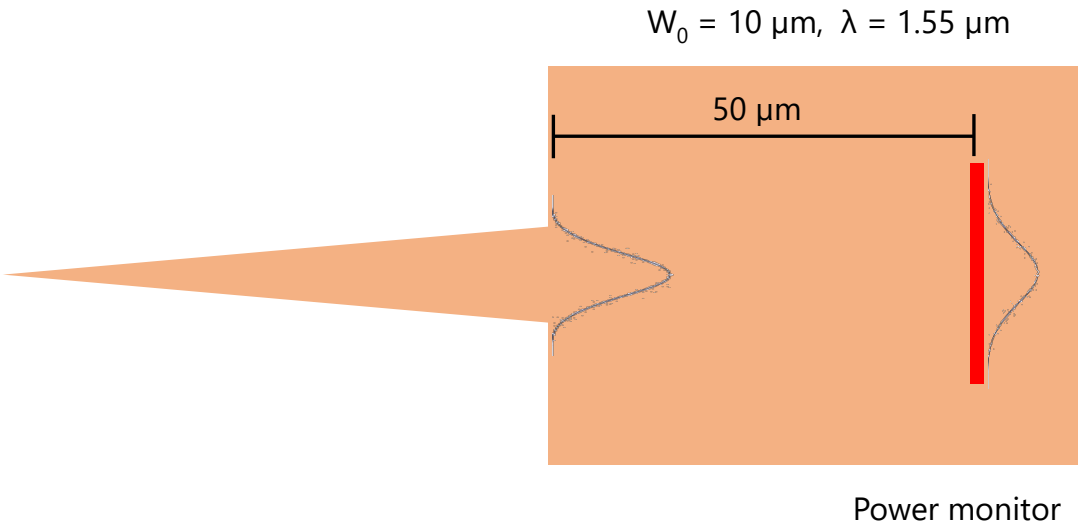

Figure 11. The taper design on the slab waveguide

The width of the FWHM usually determines the height of optical power in a spectrum, so the conditions where the smallest FWHM is the optimum condition for optical power. In the simulation of taper length variation, the optimal taper length can be determined by observing the FWHM width. The results in Fig. 11 show that for a taper length of 125 µm and thereafter, the measured FWHM width

is the narrowest value. So, in this case the taper length value of 125 μm is the minimum length for the taper to provide maximum optical power. Taper length values that are longer than 125 μm also indicate maximum optical power as well, but the longer taper conditions do not provide spatial efficiency values in a waveguide. So the optimum condition is obtained when the taper length is short but give the optimum power.

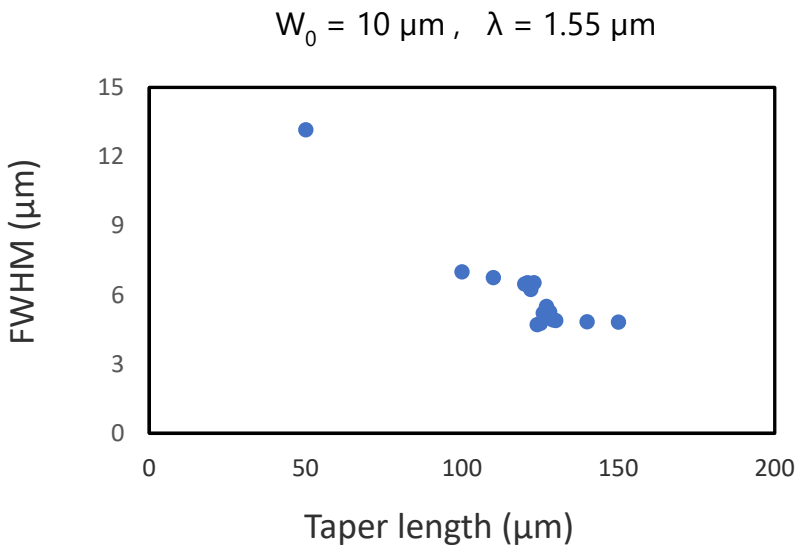

Figure 12. The dependence of FWHM on the taper length, FWHM is represent of the optical power on that position.

3.2.2. Mirror design

The light is needed to be reflected in the slab waveguide. One of reflecting mechanism to guide the light is by using mirror. The mirror's function is to reflect all incident light that propagates in slab waveguide. Our proposed design of the mirror adapted curvature with certain radius as shown in Fig. 13. The curvature design follows the concave mirror rule, that has focus point half of radius.

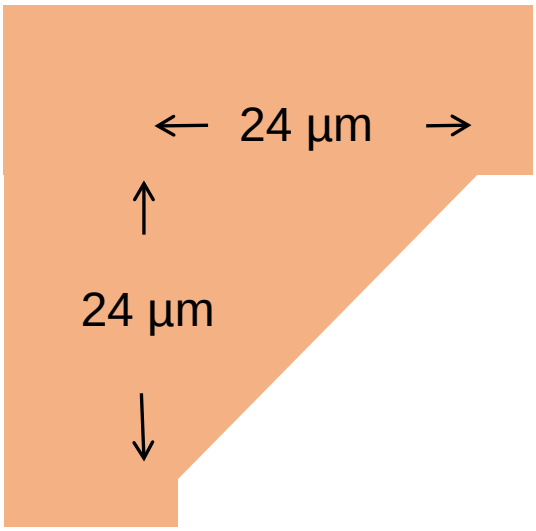

(a)

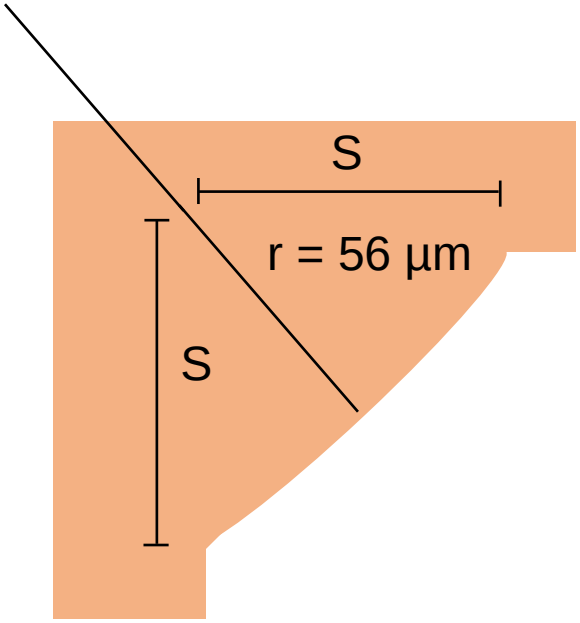

(b)

Figure 13. The mirror design on the slab waveguide. (a) flat mirror design, flat design in 45^{o} position. (b) curve mirror design has a certain radius.

The radius (*R*) of the mirror should be correlated with the distance between the two mirrors. The radius of the mirror is 110 µm and the width (*S*) of the mirror is 24 µm. The distance between two mirrors are varied to be 50 µm, 100 µm, and 200 µm. By these dimensions, the performance of the mirror is expected to be optimal. Furthermore, the performance of this mirror is measured by the mirror loss.

As an explanation in Fig. 12, the beam profile of the optical power can be estimated in width, both at the position immediately after the taper design or at a certain distance (in the order of μm). Furthermore, for the distance between mirrors 50 μm, 100 μm and 200 μm the beam profile width of the optical power can be calculated. The simulation results show that the beam profile width of the optical power at the position immediately after the taper design is 10 μm and at a distance of 200 μm by 16.5 μm. The face width of the mirror (S) is 24 μm, this value is expected to be able to capture all of the incident light coming to mirror.

The curve mirror should be correlated with the distance between the two mirrors as shown in Fig. 8. By using the curvature radius 110 μm of the first mirror, the light will collide at the reflection focus point that coincides with the second mirror precisely. The determination of the curve mirror radius is largely determined by the distance between the two mirrors. The concept of the curve mirror follows the concave mirror rule, where the reflex focus point is a half of the curvature radius. In this case, because of the curve mirror is on the material, so that the reflex focus point will be influenced by the refractive index of the material.

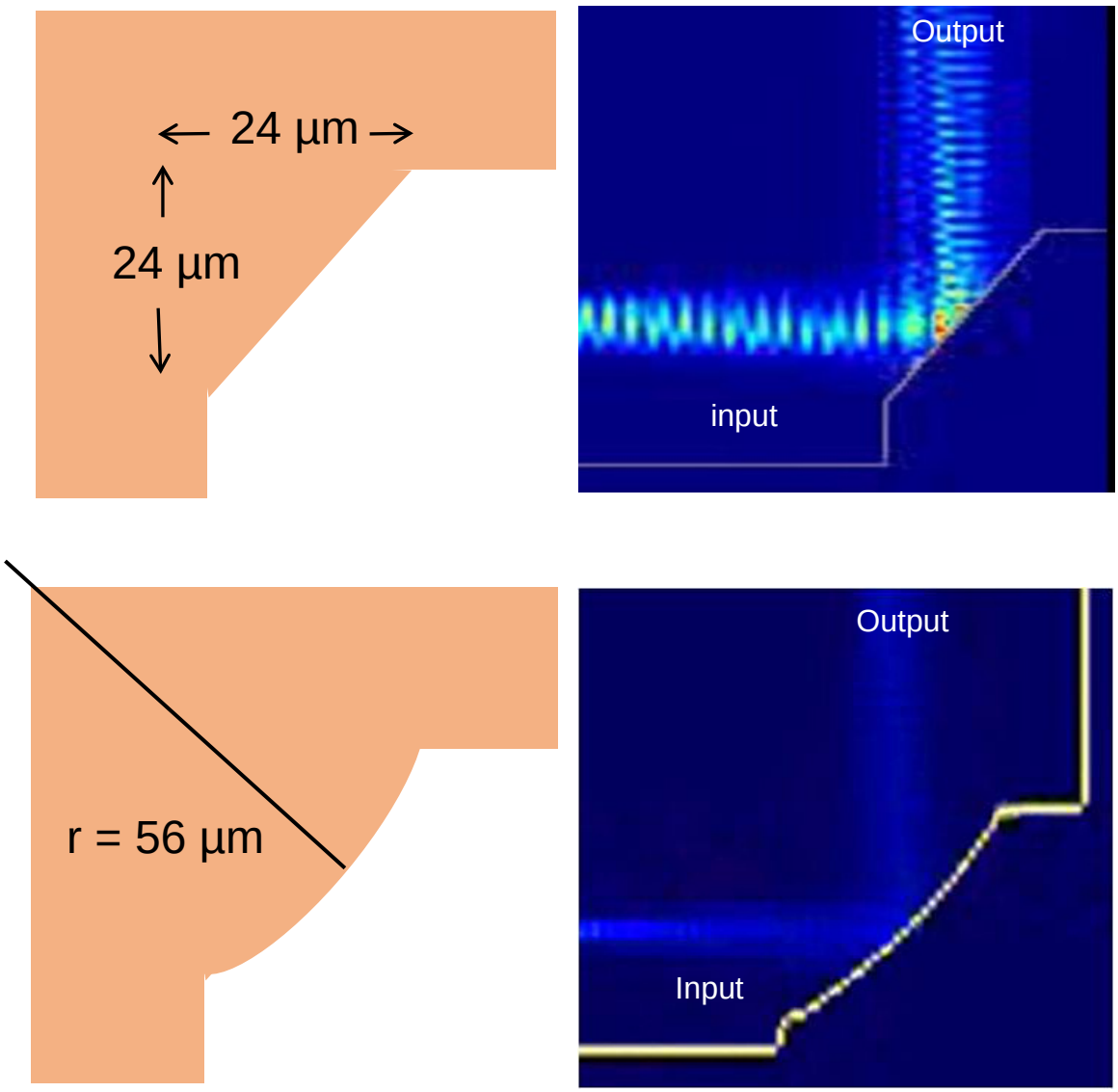

Figure 14. The mirror design and simulation result on the slab waveguide. (a) flat mirror design, (b) curve mirror design has a certain radius.

On the other matter, as can be seen from Fig. 14, the reflected light of the curvature mirror has narrower beam than the reflected light of the flat mirror. In this case, the curvature mirror might be used to reduce the mirror loss that occurs on the second mirror and the other mirrors. From the Fig. 14, the purpose of using the curve mirror design at the first mirror in a waveguide slab can reduce the potential loss of the 2^{nd}, 3^{rd} mirror etc. As follows the previous explanation, the curvature radius width will affect the reflex focus point of the mirror. So that, the position of the second mirror should be placed twice the distance of the reflex focus point on the first mirror, likewise for the third mirror and so on will be greatly influenced by the curvature radius of the previous mirror. Based on the simulation results in Figure 14, we decided the curved mirror design to fabricate. Then will measure the characteristics by the experiment.

Furthermore, we determine the characteristics of the curved mirror by simulation. The characteristics determination is represented by the mirror loss. Basically, the concept of measuring mirror loss in simulations is comparing the optical power on the position before mirror and after the mirror as shown in Figure 15. In this simulation, the power monitor size that positioned before and after the mirror is to be the same size, even in different positions.

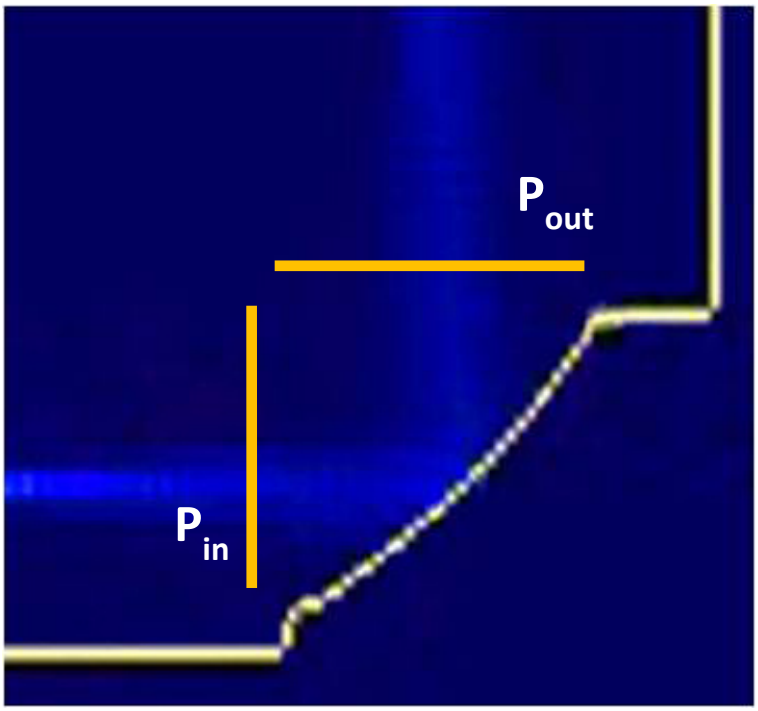

Figure 15. Simulation result of the curved mirror, power monitor

The purpose of this research is determining the optical properties of a slab waveguide, and one of the parameters measured is mirror loss, therefore the mirror loss value is very important. We do the simulations with FDTD software to compare the value of mirror loss which obtained from the experiments. In this simulation, the mirror loss is obtained by the monitor power that is placed before and after the mirror. The calculation formula follows equation 5.1.

3.2.1 Half-mirror design

The half-mirror is an optical device that splits a beam of light in two of part. It is a crucial part of many optical experimental and measurement systems, such as interferometers, also finding widespread applications in fiber optic telecommunications. Usually the beam splitter is made of cube with a thin layer positioned 45^{o}, after passing through the cube, half of the light incident through one "port" is reflected and the other half is transmitted due to frustrated total internal reflection (FTIR). The amount of optical power that is split in the beam splitter depends on the thickness of a thin layer.

The concept of the beam splitter cube should be implemented in the slab waveguide, that is adding a thin layer whose refractive index is lower than the refractive index of the slab waveguide. The angel position of the thin layer must be greater than the critical angle, so it is assumed that all of the incident light will be reflected perfectly, but because of the thickness of the layer is very thin, some power will penetrate and through the thin layer. That is consequence of the FTIR phenomena.

In this research we propose SiO_2 as a thin layer material, the refractive index of SiO_2 is 1.47. In here, the half-mirror in a waveguide slab is consist of the Si as the waveguide and SiO_2 as a thin layer. The SiO_2 with the certain thickness is needed, while the length of the SiO_2 is expected to capture all of the incident light coming to the mirror as shown in Fig. 16. The refractive index material was chosen as thin layer must be lower than the waveguide refractive index, this argue is refers to the Snellius law of reflection at the flat surface on two different materials.

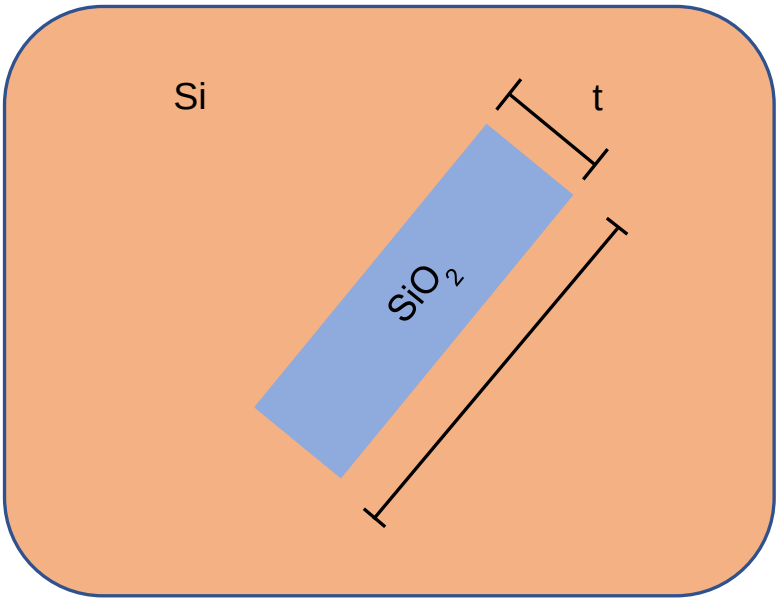

Figure 16. The half-mirror design on the slab waveguide, the half-mirror consists of the Si as the waveguide and SiO_2 as the thin layer.

The FDTD simulation software is used to check the half-mirror concept in the slab waveguide. The initial hypothesis that has been explained before can be proven by the top view image of the simulation results. As shown in the Fig. 17, the incident light which coming towards to the thin layer will be divided become two part, one of the propagations is continue in the same direction while others will be reflected on the 90^{o} direction. Referring to the Fig. 16 also, the reflected propagation after passing through the thin layer is thicker and saturated. These phenomena show about the power monitor in simulation is counted twice, that is incident light coming from the light source and propagation after passing through the thin layer.

The half-mirror is very possible to be applied in various applications such as interferometer, both the concept of Michelson interferometer and Mach-Zander Interferometer. The half-mirror split the propagation becomes two and then reflect it to the mirror, on the other hand, the half-mirror also can combine the two propagation becomes one spectrum in the output of interferometer. Furthermore, the application of the half-mirror concept in the slab waveguide makes it possible to develop the interferometer in the slab waveguide.

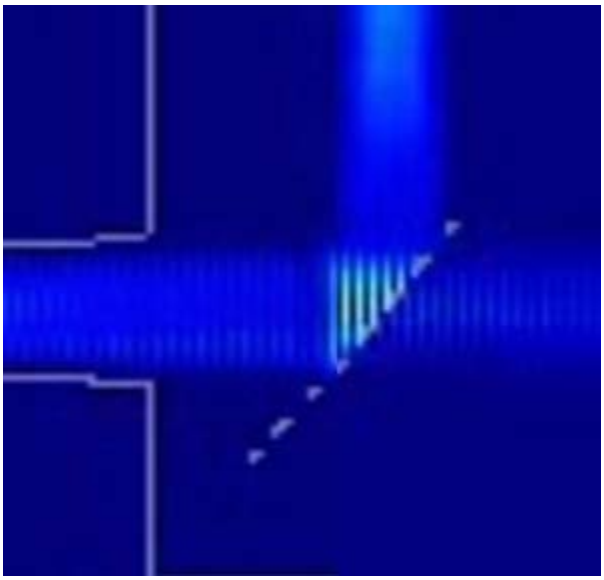

Figure 17. The simulation result of the half-mirror design on the slab waveguide, the incident light will be split after through the thin layer.

After we propose a model of the half-mirror on the slab waveguide, then we determine the amount of optical power that is divided after through the thin layer. The amount of optical power which reflected or transmitted is depends on the thickness of the thin layer. Furthermore, we determine the conditions of 50% reflected and 50% transmitted after splitting. When the thickness of the thin layer is too thick, then the percentage of reflected power will be greater than the transmitted percentage, otherwise when the thin layer is too thin, almost all of optical power comes to pound the thin layer will be transmitted. The concept of

how to determine the thickness of the thin layer in 50-50 conditions of reflected and transmitted power as shown in Figure 18. In that figure, it is assumed that the thickness of a thin layer (*t*) is devide the optical power in reflected propagation and transmitted propagation, so that the thickness of the thin layer is very important. Moreover, the thin film mounted at an angle of 45^{o} is intended to produce reflections that are straight up against a flat surface.

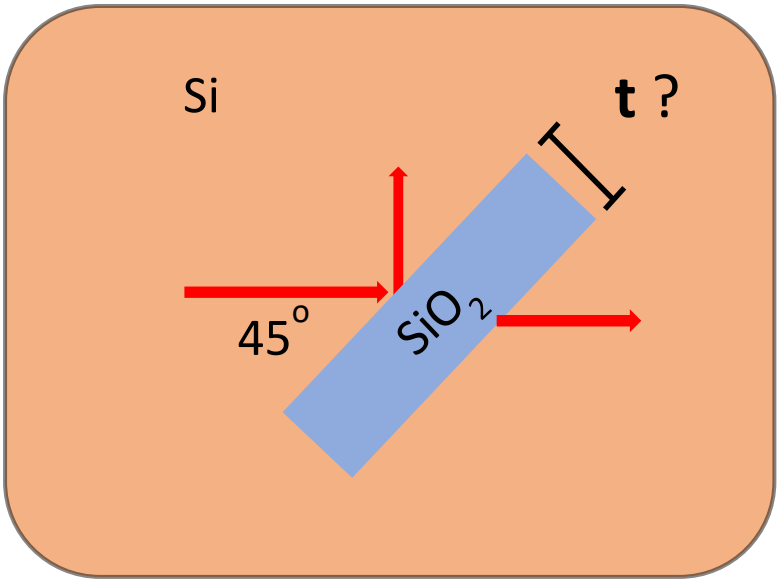

Figure 18. The simulation result of the half-mirror design on the slab waveguide, the incident light will be split after through the thin layer.

Simulation results of the thin layer thickness dependency are shown in Fig 18. In the Figure 19 (a) shows that most of the optical power is reflected after passing through the thin film, the thickness of thin film in this condition is 150 nm. So that, the 150 nm is too thick for 50-50 reflected and transmitted condition. While on the figure (b) shows the opposite, most of the optical power is transmitted after passing through thin film. In the picture condition (b) the thickness of the film is 65 nm. So that, the 65 nm is too thin for 50-50 reflected and transmitted condition. The ideal condition for obtaining 50-50 reflected and transmitted condition is using the thickness of 110 nm thin film, this phenomenon is illustrated in Fig. 18. For the detailed explanation of measuring thin layer thickness dependency will be explained in Fig.19, here, the simulation results of the thin layer thickness are accumulated in one graph, so that it can be concluded that 110 nm is suitable for 50-50 reflected and transmitted conditions.

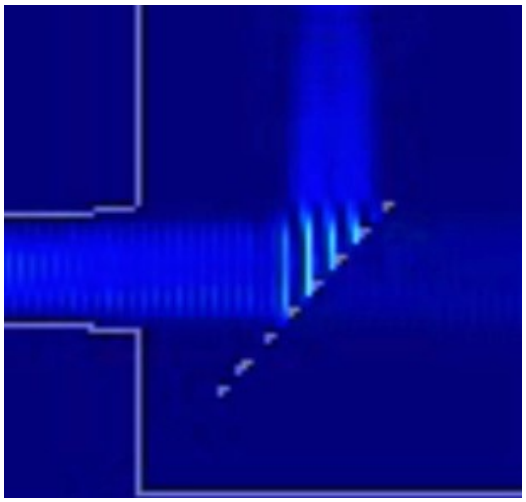

(a)

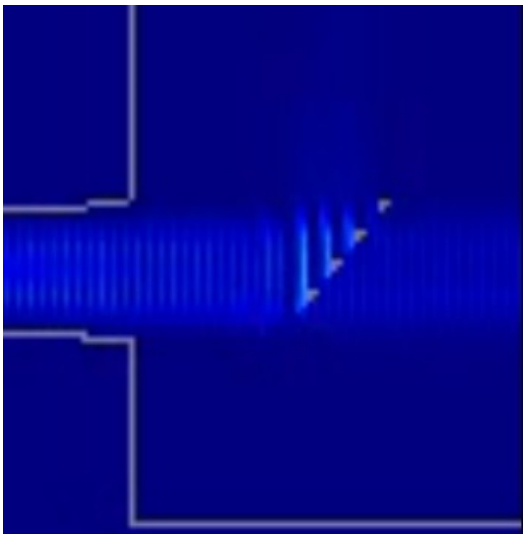

(b)

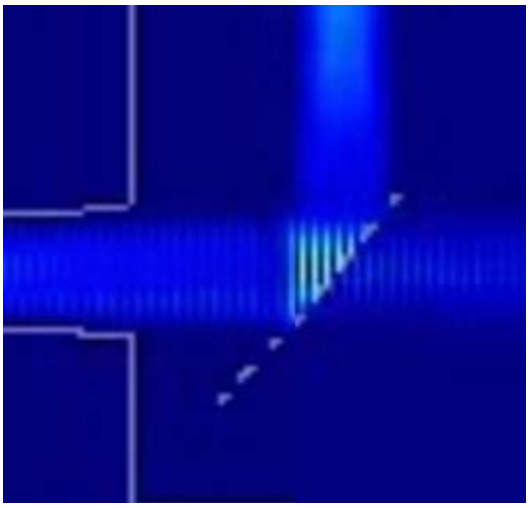

(c)

Figure 19. The simulation result of the half-mirror design on the slab waveguide, the transmitted and reflected power is strongly influenced by the thickness

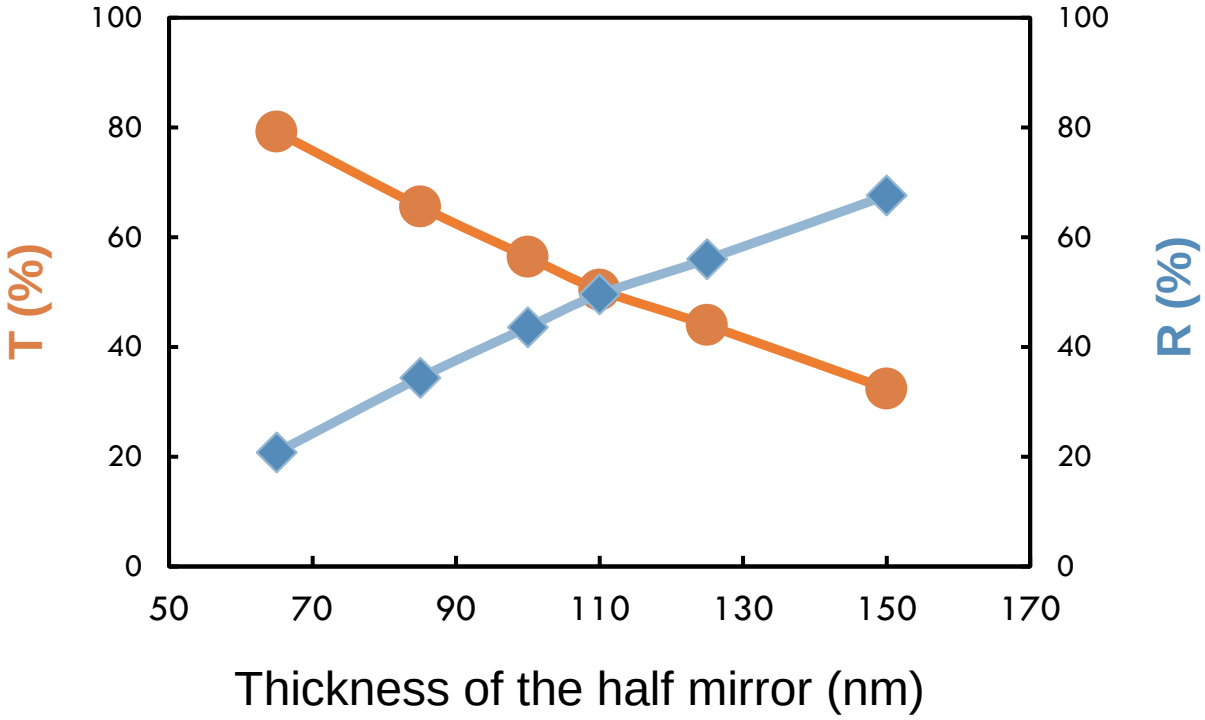

Figure 20. The transmitted and reflected power dependence on the thickness of the half-mirror in the TE polarization

Figure 20 shows about the correlation between thin layer thickness and transmitted power and also reflected power. The graph shows the measurements in TE polarization conditions. In this calculation, the value of transmitted power and reflected power was compared to the optical power before crossing the thin layer, so that the data about transmitted and reflected power is presented in percentage.

The correlation between the thin layer thickness and transmitted power is shown in the orange color chart, whereas the thickness of the thin layer increases the transmitted power decreases linearly, and the highest value of transmitted power is achieved when the thin layer thickness is lowest. Then, the thickness of thin layers was tested in 65 nm, 85 nm, 100 nm, 110 nm, 125 nm to 150 nm. While the correlation between the thickness of the thin layer to the reflected power is shown in the blue graph, whereas the thickness of the thin layer increases, the reflected power will also increase linearly. And the highest reflected power is obtained at the highest thickness of the thin layer also. From the plotting between the orange and blue graphs, 50-50 conditions can be obtained from the intersection of the two lines. From the intersection of these lines it can be calculated that the 50-50 conditions for TE polarization are obtained when the thickness of the thin layer is 110 nm.

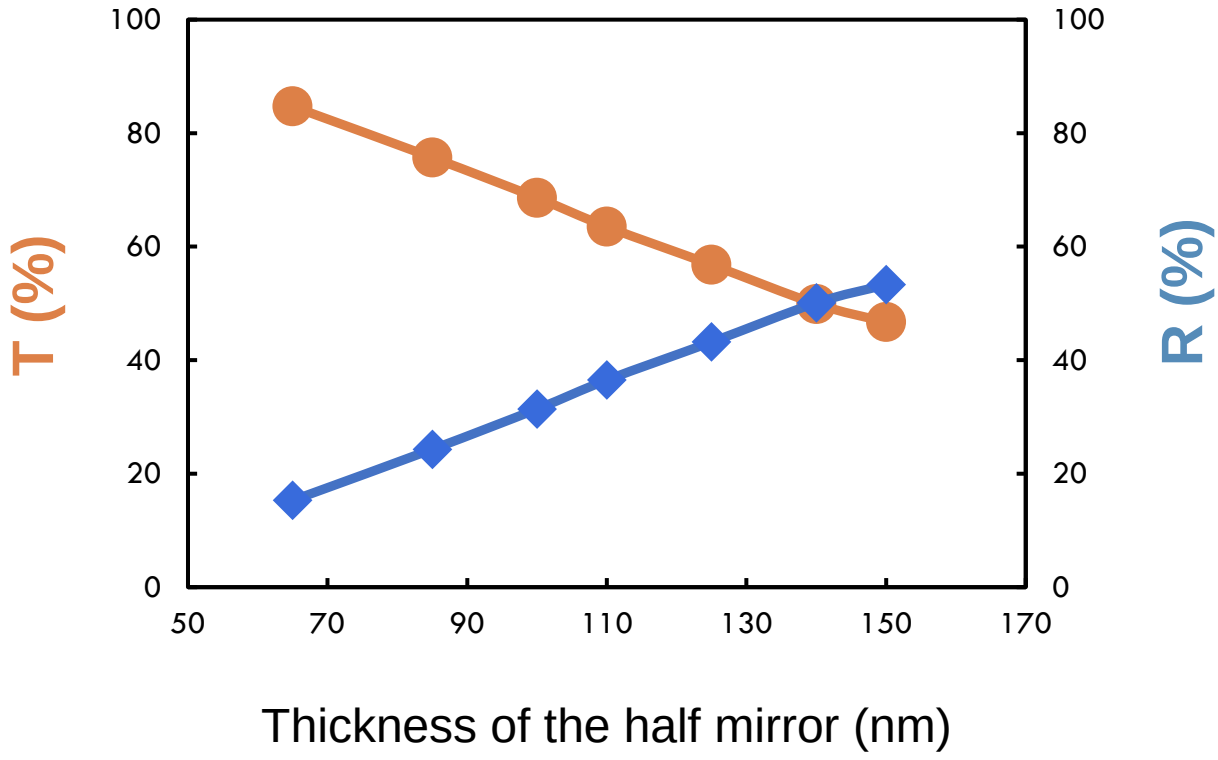

Figure 21. The transmitted and reflected power dependence on the thickness of the half-mirror in the TM polarization

Figure 21 shows about the correlation between thin layer thickness and transmitted power and also reflected power. The graph shows the measurements in TM polarization conditions. In this calculation, the value of transmitted power and reflected power was compared to the optical power before crossing the thin layer,

so that the data about transmitted and reflected power is presented in percentage. The correlation between the thin layer thickness and transmitted power is shown in the orange color chart, whereas the thickness of the thin layer increases the transmitted power decreases linearly, and the highest value of transmitted power is achieved when the thin layer thickness is lowest. While the correlation between the thickness of the thin layer to the reflected power is shown in the blue graph, whereas the thickness of the thin layer increases, the reflected power will also increase linearly. And the highest reflected power is obtained at the highest thickness of the thin layer also. From the plotting between the orange and blue graphs, 50-50 conditions can be obtained from the intersection of the two lines. From the intersection of these lines it can be calculated that the 50-50 conditions for TM polarization are obtained when the thickness of the thin layer is 140 nm. The difference in thickness required to achieve 50-50 conditions in TE and TM polarization is due to the different characteristics of the two polarization. According to the reflectance reference, the TM polarization is higher than the TE polarization for all reflection angles.

3.2.4 Retroreflector design

A retroreflector is a device or surface that reflects radiation (usually light) back to its source with minimum scattering. In a retroreflector the wave front of the radiation is reflected straight back to the wave's source. This works at a wide range of angle of incidence, unlike a planar mirror, which does this only if the mirror is exactly perpendicular to the wave front, having a zero angle of incidence. In this research, we propose a retro reflector design in the slab waveguide. The retro reflector is made by the material with the refractive index lower than the waveguide refractive index. In this case, we propose SiO_2 with the refractive index is 1.47 for a wavelength of 1550 nm.

The retroreflector concept is usually applied in Michelson interferometers. In this concept, the light propagation that come into the retroreflector mirror is reflected perfectly in the opposite direction. Moreover, the application of retroreflector in the slab waveguide requires special conditions. The flat mirror cannot be used as a retroreflector in the slab waveguide, because the flat mirror cannot reflect only in one direction. We propose to use the elbow mirror as shown in Fig. 22.

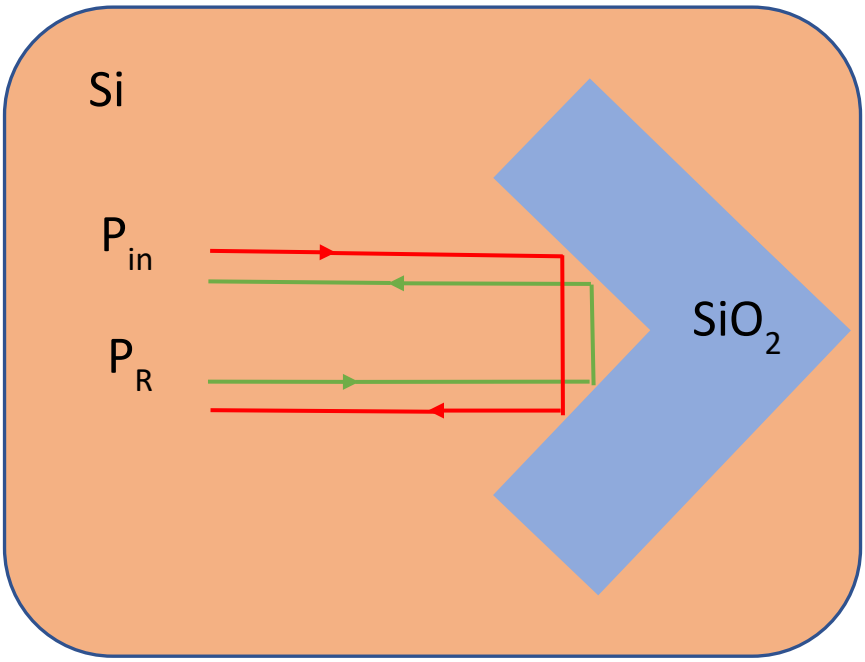

Figure 22. The concept of the retroreflector in the slab waveguide

As shown in Figure 22, the design of an elbow mirror as a retroreflector has return all of the light propagations that come to the mirror. Referring to the red line on the Fig. 22, that comes to the elbow mirror, then the red line is returned in the opposite direction. On the other hand, the green line shows the opposite direction to comes to the elbow mirror, but the green line also undergoes the same process. The retroreflector on the slab waveguide consists of the SiO2 as the material of the elbow mirror with a refractive index is 1.47 for a wavelength of 1550 nm.

3.3 Integrated the design

After we explain some designs in detail, some of these designs are seen from Fig. 9 until Fig. 14. Then some of these designs can be integrated in a new design that includes the functions of each previous design. The integrated design describes the characteristic of the slab waveguide.

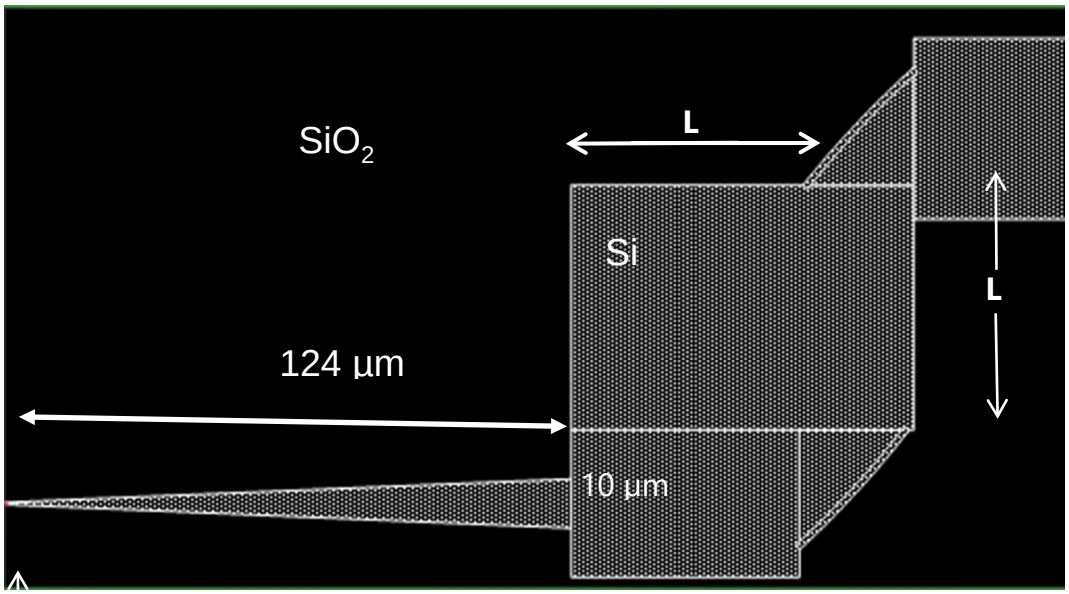

Figure 23. The concept of the integrated design in the slab waveguide

Figure 23 illustrates the light propagation in the slab waveguide. It is shown that the light propagation can be detected at the long-distance, even though the light propagation is not straight, but is bent. In the simulation, the power analysis is obtained by putting a power monitor. By analyzing the power monitor before and after mirror positions, the mirror loss can be obtained. Meanwhile, the propagation loss can be obtained by positioning the power monitor in slab waveguide without other components inside.

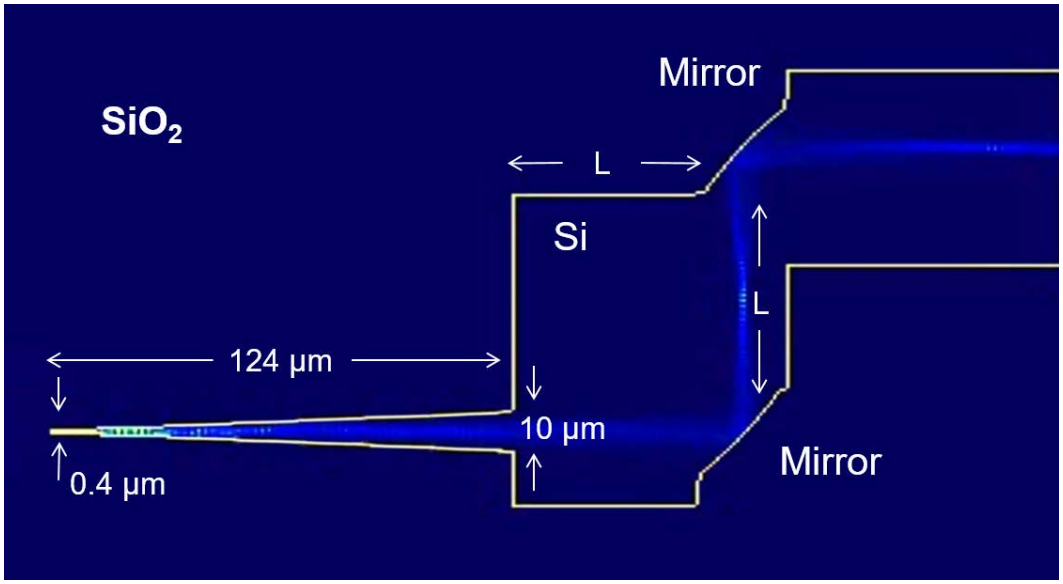

Figure 24. The simulation result of the integrated design, that design includes the taper design and the curved mirror design.

Meanwhile, the integration of several designs consisting of the taper design, the half-mirror design and the retroreflector design is carried out to check the quality of the slab waveguide. The details of these designs as described in Figure 16 until Figure 22. The combination of these designs is create new design such as the Michelson Interferometer.

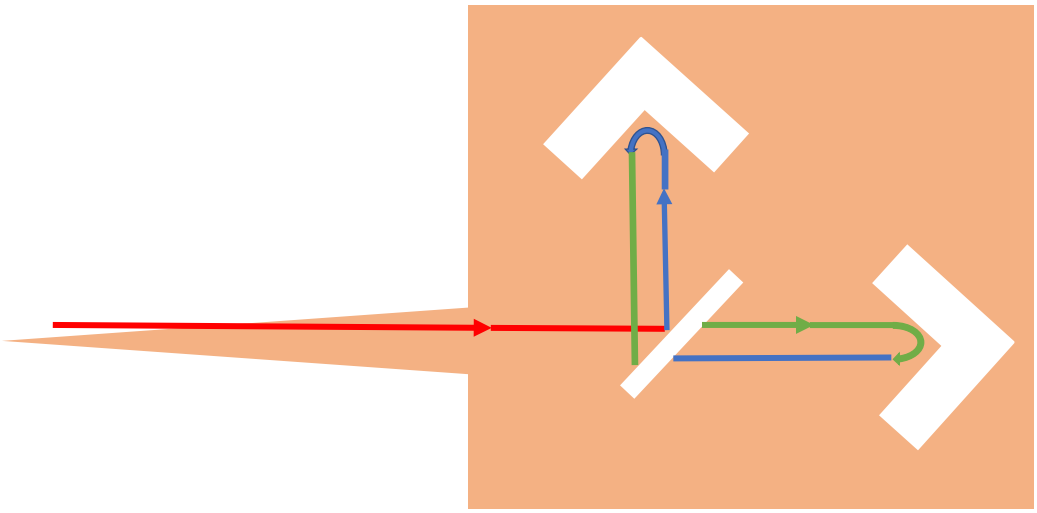

Figure 25. The concept of the integrated design in the slab waveguide, that design includes the taper design, the half-mirror design and the retroreflector design.

Figure 25 illustrates the combination of several designs that have been discussed in detail before. We illustrate the light propagation coming from the end of the taper design, this is indicated by the red line. Then the propagation light collides the half-mirror which will split into two propagation light, one propagation light is transmitted and the other one is reflected. The transmitted and reflected light is illustrated by the green line. Moreover, the results of reflection and transmission is moving straight until it collide a retroreflector, and the retroreflector is reflecting all of the propagation light that come in the opposite direction.

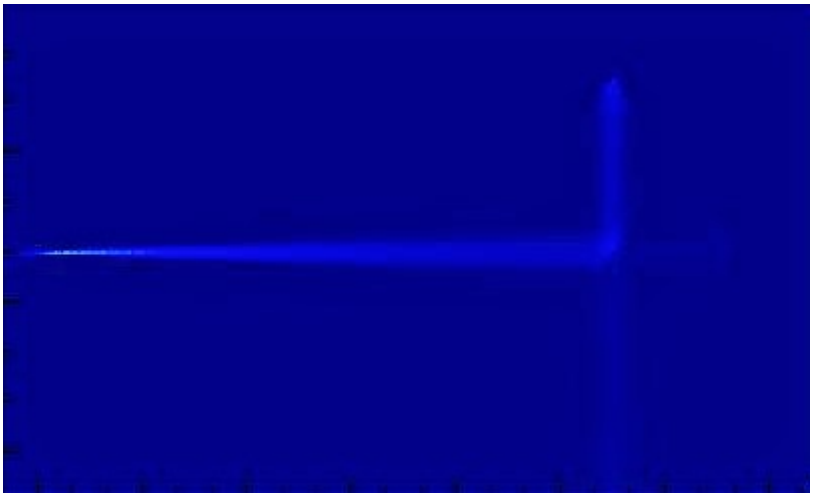

Figure 26. The simulation result of the integrated design, that design includes the taper design, half-mirror design and the retroreflector.

Figure 26 illustrates that the half-mirror can split the propagation light evenly. This illustrates also shows the optical power is divided into 50% transmitted and 50% reflected. The simulation results show that optical power is represented by the light blue color, while the slab waveguide is represented in dark blue as the background.

3.6 Potentially loss on the system

In an optical waveguide system, it is necessary to know about the comparison of the optical power before entering the optical waveguide and the optical power after passing through the optical waveguide. This comparison can indicate the quality of the slab waveguide. The percentage of the optical power in a slab waveguide is usually called as the optical loss. When the slab waveguide slab has the low optical loss, so that the quality of the slab waveguide is very good. And vice versa when there is a lot of optical loss in the slab waveguide, then there might be a mistake in the design, material selection or mismatch the position.

In this section, we discuss the potential loss in the slab waveguide system. By using an integrated design as shown in Figure 23, we describe some optical losses that may occur in the system as shown in Figure 27.

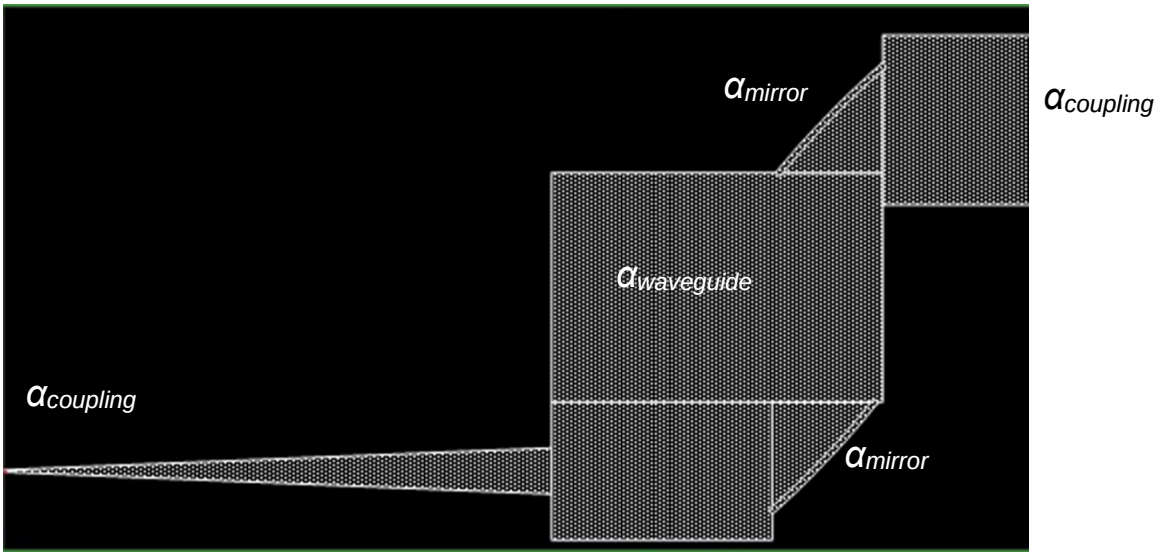

Figure 27. The potentially loss in the slab waveguide system.

Chapter 4

Experimental Set up

4.1 Fabrication by foundry service

In silicon photonics toward the realization of optical interconnects, Si can be used as a photodetector for communications in the 0.8 μm band. According to this method, the Si photodetector and the electronic circuit can be manufactured by the same process, and the steps of physical connection between the electronic circuit and the light receiving element substrate and electrical connection by wire bonding become unnecessary.

The attraction of silicon photonics is low cost and high yield of device fabrication due to the excellent optical characteristics of Si and high compatibility with existing CMOS processes. However, there is another major attraction in silicon photonics: the use of foundries with advanced process technology, especially CMOS foundries. The CMOS Foundry will use large-scale facilities for manufacturing electronic circuits to produce chips with integrated optical devices.

Since production is performed using an acceptable recipe, device design is greatly restricted, but devices can be produced at low cost. A multi-user wafer plan is also possible, in which the fabrication of optical devices from multiple laboratories on the same chip reduces the burden of mask costs per laboratory. Also in the device fabrication, there is an advantage that much higher precision, uniformity, and large-scale integration can be realized as compared with original fabrication. Therefore, in recent years, many research institutes have manufactured optical devices using foundry services.

This laboratory also manufactures optical waveguides and photodetectors using the foundry service. In this chapter, we will explain the fabrication of Si photodetectors using the foundry service. Research institutions offering foundry services include IME (Singapore), IMEC (Belgium), NTT-AT (Japan), and ST Microelectronics (France). Among them, IME's foundry service is used in this research. In this foundry service, multiple research institutions are involved in the same wafer, and Professor Toshihiko Baba of Yokohama National University plays a central role in ordering once a year.

4.1.1 Fabrication flow

The following shows the flow of chip fabrication using IME's foundry service.

1. Design the chips that you want to make in each research institute by 2D CAD. In this study, we used VDEC tools (Custom IC Design Tools, Cadence) for CAD design and designed based on the sample of GDS file sent from IME. Chip making recipes and chip sizes may change from year to year, and some layers may not be usable in certain years.

2. The designed CAD is output as a GDS file and uploaded to the FTP link specified by IME. Unlike IC fabrication through VDEC, there is no rule check, but there is a limit to the line width that can be fabricated. Masks can be of high or low accuracy. The former is used to fabricate key components of silicon photonics such as Si, while the latter is used for electrodes, heaters, windows, trenches, etc. The former compensation is greater than 200 nm and the latter is greater than 1 μm.

3. The IME roughly checks the CAD and corrects data and adds data for mask alignment as needed. Download the GDS file modified by IME from the specified URL, receive it at each research institution, and perform a final check.

This is the last time data can be modified, and the modified GDS file by the deadline is uploaded to an FTP link.

4. IME creates a mask based on the GDS collected from each research institute and creates devices on the wafer. The fabricated device is divided into chips by dicing, and a plurality of chips are sent to respective laboratories. Chips may be sent multiple times. For example, when ordering both a passive device and an active device, a chip in which only the passive device is integrated arrives first, and then a chip in which the active device is also integrated arrives. If there is a complaint for the manufactured chip, the chip may be re-manufactured and newly delivered.

4.1.2 Experimental set up for the propagation loss

Propagation loss measurements are done by inserting input light from a laser source into the optical slab waveguide. The polarizing maintenance fiber (PMF or PM fiber) is use which is connected from the fiber lens to input the laser into the input port of slab waveguide. By using PMF, it will ensure the propagation of polarized light is in the same direction. PMF is a single-mode optical fiber in which linearly polarized light, if properly launched into the fiber, maintains a linear

polarization during propagation, exiting the fiber in a specific linear polarization state; there is little or no cross-coupling of optical power between the two polarization modes. Note that a polarization-maintaining fiber does not polarize light as a polarizer does. Rather, PM fiber maintains the linear polarization of linearly polarized light provided that it is launched into the fiber aligned with one of the fiber's polarization modes. Launching linearly polarized light into the fiber at a different angle will excite both polarization modes, conducting the same wave at slightly different phase velocities. At most points along the fiber the net polarization will be an elliptically polarized state, with a return to the original polarization state after an integer number of beat lengths. Consequently, if visible laser light is launched into the fiber exciting both polarization modes, scattering of propagating light viewed from the side, is observed with a light and dark pattern periodic over each beat length, since scattering is preferentially perpendicular to the polarization direction.

In here, the fiber lens can minimize the coupling loss at the input port of slab waveguide due to the difference between the size of the input port and PMF. Lensed fiber is produced using different fine lens tip shaping techniques. Each micro-lens characterized using: far optical field and near optical field analysis, return loss,

working distance measurements and geometrical measurements. Cone lenses: are cylindrical rod lenses with one end worked into a conical surface. The circumference of the rod is typically ground whereas the conical element is polished. This makes the lens ideal for 360º illumination, laser and imaging systems.

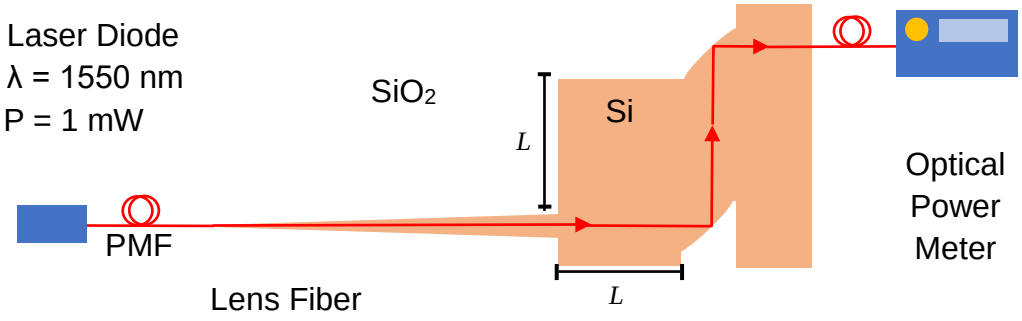

Figure 28. The experimental setup of the propagation loss measurement in the slab waveguide.

A tunable laser is a laser whose wavelength of operation can be altered in a controlled manner. While all laser gain media allow small shifts in output wavelength, only a few types of lasers allow continuous tuning over a significant wavelength range. The first true broadly tunable laser was the dye laser in 1966. Hänsch introduced the first narrow-linewidth tunable laser in 1972. Dye lasers and some vibronic solid-state lasers have extremely large bandwidths,

allowing tuning over a range of tens to hundreds of nanometers. Titanium-doped sapphire is the most common tunable solid-state laser, capable of laser operation from 670 nm to 1,100 nm wavelength. Typically these laser systems incorporate a Lyot filter into the laser cavity, which is rotated to tune the laser. Other tuning techniques involve diffraction gratings, prisms, etalons, and combinations of these. Multiple-prism grating arrangements, in several configurations, as described by Duarte, are used in diode, dye, gas, and other tunable lasers.

A schematic of a generic tunable laser together with the relative spectra of the necessary filter and gain elements as well as the location of the various cavity modes that all must be properly aligned and translated to create a tunable, single-frequency laser. Of course, in most practical embodiments. Transparent optical space switch composed of a wavelength converter array and a passive router such as an arrayed-waveguide-router (AWG). Line cards with tunable lasers can more generally be replaced by wavelength converters. filter, mirror and phase-shifting elements are combined in some way to create a unique physical structure for the different kinds of tunable lasers. It can be used to see how a tunable semiconductor laser evolves from the most basic “Fabry-Perot” laser, which has just the gain and the two simple mirror elements, to a “single-frequency” laser, which adds the

mode-selection filter, to a “tunable single-frequency” laser, which adds possible adjustment of the mirror position and the center frequency of the mode-selection filter, as well as adding a new adjustable cavity phase element. For more analytical discussion, the reader is referred to be.

An optical power meter (OPM) is a device used measure the power in an optical signal. Optical Meters are benchtop or handheld instruments used to measure properties of light like power, energy, or wavelength. The term usually refers to a device for testing average power in fiber optic systems. Other general purpose light power measuring devices are usually called radiometers, photometers, laser power meters. Optical power meter responds to a broad spectrum of light, however, the calibration is wavelength dependent. This is not normally an issue, since the test wavelength is usually known, however, it has a couple of drawbacks. Firstly, the user must set the meter to the correct test wavelength, and secondly, if there are other spurious wavelengths present, then wrong readings will result.

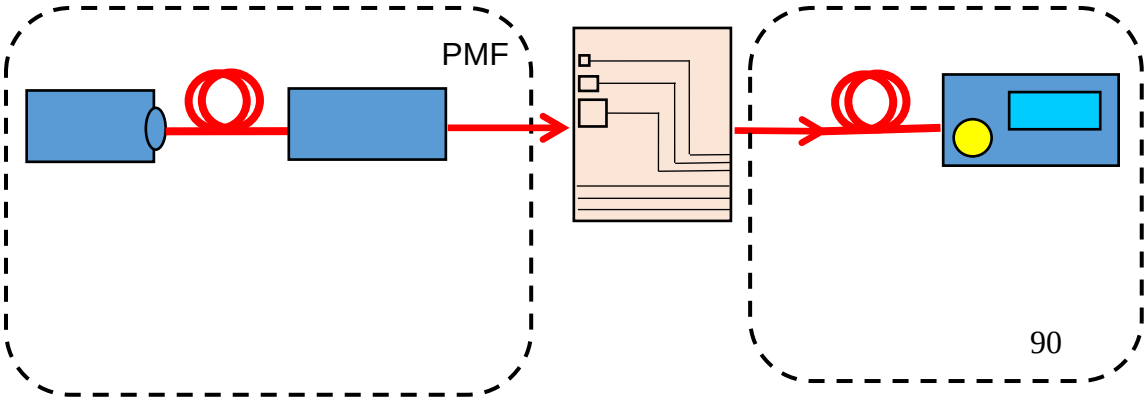

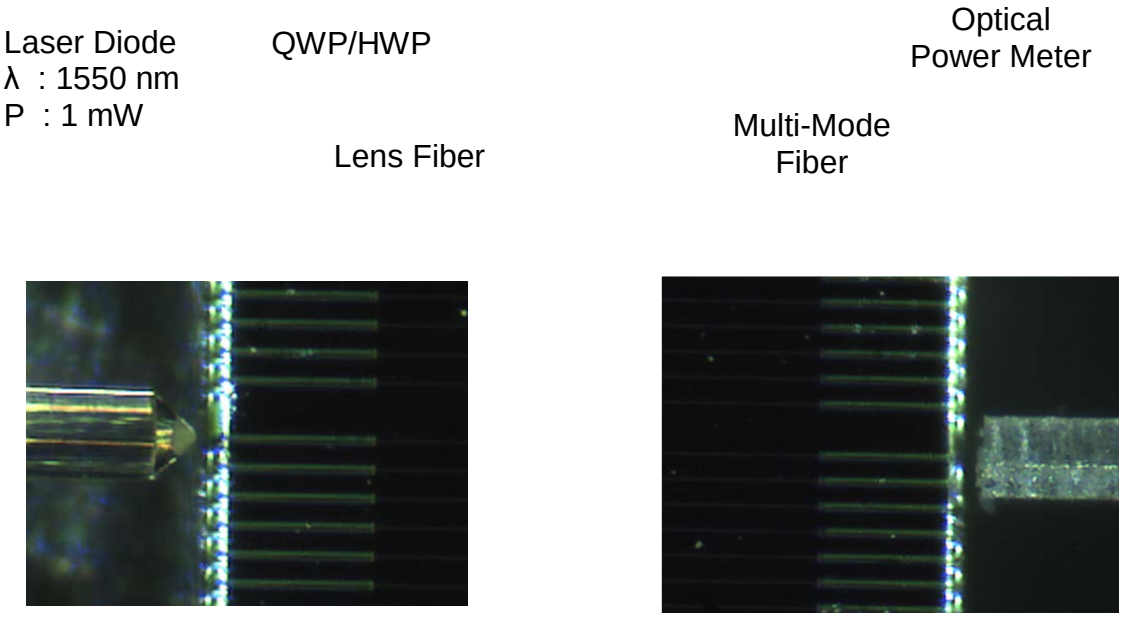

Figure 29. The measurement component in the input port and the output port.

Wave plates, also known as retarders, transmit light and modify its polarization state without attenuating, deviating, or displacing the beam. They do this by retarding (or delaying) one component of polarization with respect to its orthogonal component. A retarder is an optical device that alters the polarization state of a light wave travelling through it. Two common types of wave plates are the *half-wave plate* (HWP), which shifts the polarization direction of linearly polarized light, and the *quarter-wave plate* (QWP), which converts linearly polarized light

into circularly polarized light and vice versa. A quarter-wave plate can be used to produce elliptical polarization as well. In unpolarized light, wave plates are equivalent to windows – they are both flat optical components through which light passes. Wave plates are made from birefringent materials, most commonly crystal quartz. Birefringent materials have slightly different indices of refraction for light polarized in different orientations. The TE-TM mode propagation is produced by rotational wave plate, which is included half wave plate (HWP) and quarter wave plate (QWP). The output mode of the light source is only in one mode propagation after pass through the rotation wave plate.

Multi-mode optical fiber is a type of optical fiber mostly used for communication over short distances, such as within a building or on a campus. Multi-mode links can be used for data rates up to 100 Gbit/s. Multi-mode fiber has a fairly large core diameter that enables multiple light modes to be propagated and limits the maximum length of a transmission link because of modal dispersion. Multi-mode fiber is also used when high optical powers are to be carried through an optical fiber. The main difference between multi-mode and single-mode optical fiber is that the former has much larger core diameter, typically 50–100 micrometers; much larger than the wavelength of the light carried in it. Because of

the large core and also the possibility of large numerical aperture, multi-mode fiber has higher "light-gathering" capacity than single-mode fiber. In practical terms, the larger core size simplifies connections and also allows the use of lower-cost electronics.

The incident light will propagate into the slab waveguide and directed by the mirror. The measurement is done for several chips of slab waveguide with variation of the number of mirrors such as 2, 4 and 6 mirrors. The next measurements are variations in path length, the distance between two mirrors (L) and the distance between the position after taper and first mirror, which is set to be 50 µm, 100 µm and 200 µm in slab waveguide design. In this measurement, tunable semiconductor laser with wavelength of 1550 nm and output power of 1 mW is used as a light source.

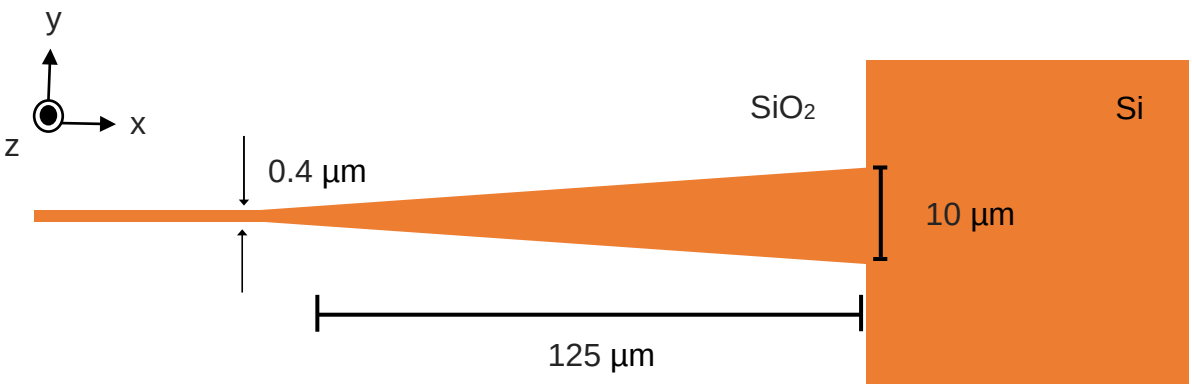

Figure 30. The optical waveguide design consists of the channel waveguide, linear taper and slab waveguide.

The total loss that occurs in a slab waveguide includes coupling loss, which is losses at the input and output port of slab waveguide due to the difference between the size of optical fiber to and from input and output port of slab waveguide. The other loss is waveguide loss, that is loss when the light propagates in slab including the mirror loss, which is loss when the light is reflected at the mirror.

Chapter 5

Result and Discussion

5.1 Experimental result

Based on our design, the slab waveguide is fabricated and the total loss in slab waveguide including coupling loss, waveguide loss, and mirror loss is calculated by Eq. 5.1:

$$Total\ loss = 10\ log\ \frac{P_{out}}{P_{in}} \tag{5.1}$$

Where P_{out} and P_{in} are the output and input optical power of the slab waveguide in the experiments. Then the data are classified based on the number of mirrors as shown in Fig. 31. The experimental results are also shown on the TE and TM propagation mode. In this case, total loss is the total amount of loss from net waveguide loss, mirror loss and coupling loss.

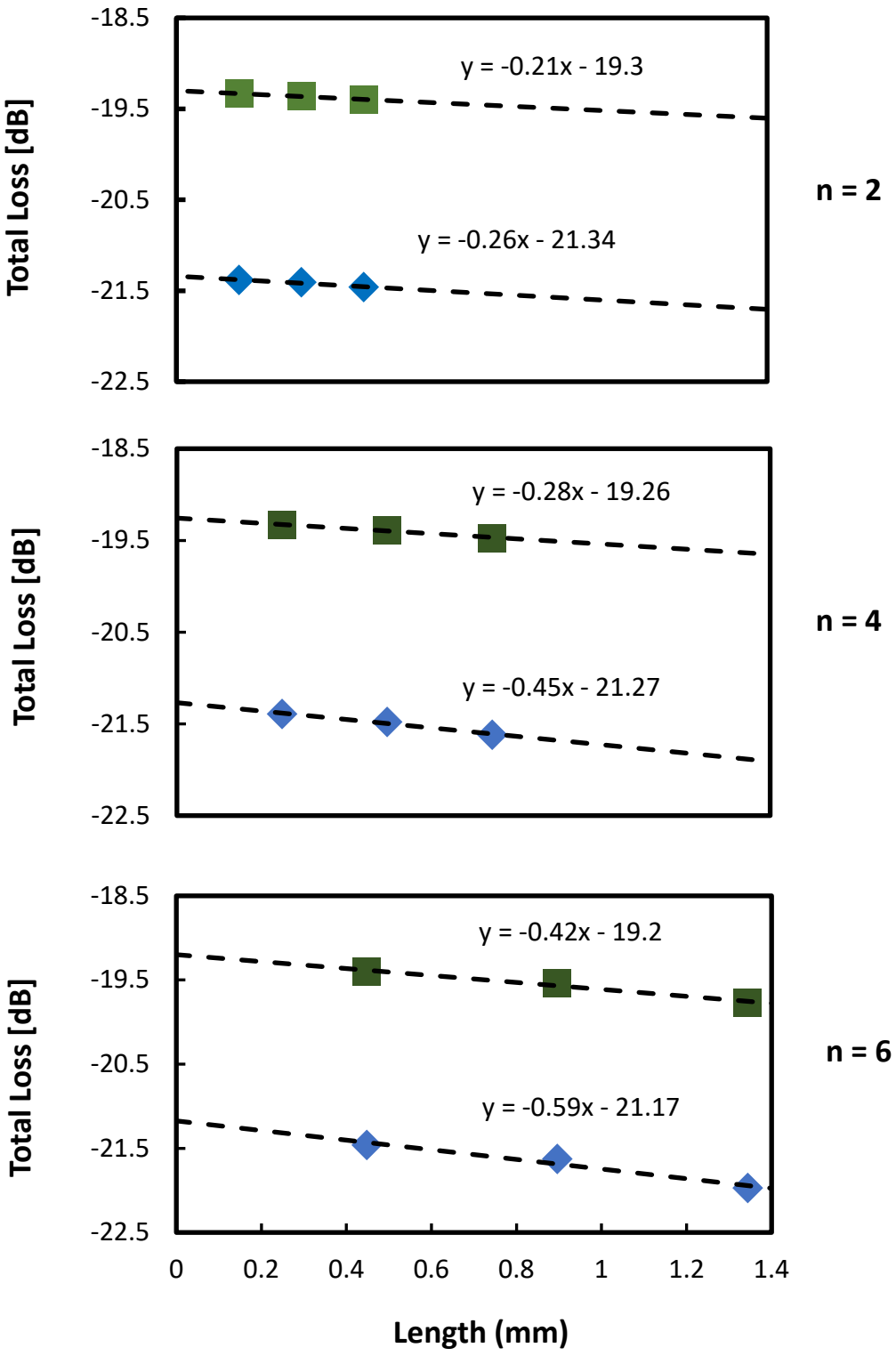
-18.5
-19.5
-20.5
-21.5
-22.5
Total Loss [dB]
y = -0.21x - 19.3
y = -0.26x - 21.34
n = 2
y = -0.28x - 19.26
y = -0.45x - 21.27
n = 4
y = -0.42x - 19.2
y = -0.59x - 21.17
n = 6
0
0.2
0.4
0.6
0.8
1
1.2
1.4
Length (mm)

Figure 31. The dependence of total loss on the waveguide length in the slab waveguide. “n” is the number of mirrors. and are the TE and TM polarizations, respectively.

The total waveguide length can be calculated as the total length between mirrors and the size of mirrors itself. The total waveguide length for 2 mirrors are varied to be 148 μm, 248 μm and 448 μm for 50 μm, 100 μm and 200 μm distance between mirrors respectively. The total lengths of the waveguide for 4 and 6 mirrors in slab waveguide are 296 μm and 444 μm (for 50 μm distance between mirrors), 496 μm and 744 μm (for 100 μm distance between mirrors) and 896 μm and 1344 μm (for 200 μm distance between mirrors) respectively. From Figure 6, the coupling losses of slab waveguide with 2, 4 and 6 mirrors can be calculated on the TE mode are 21.34 dB, 21.27 dB and 21.17 dB respectively, and on the TM mode the coupling losses are 19.3 dB, 19.26 dB and 19.2 dB.

The analysis based on experiment results shows that total loss increases as the number of mirrors and distances between mirrors increase. As shown in Fig. 32, the propagation loss is strongly influenced by waveguide length and number of mirrors. Furthermore, from the experimental results, the net waveguide loss is obtained to be 0.10 dB/mm and 0.09 dB/mm on the TE and TM mode respectively.

Note that, net waveguide loss is the loss caused by the light propagation in slab waveguide and does not include mirror loss, on the other hand, in this analysis, the term "propagation loss" refers to the losses caused by the light propagation passing through the slab waveguide including mirror loss.

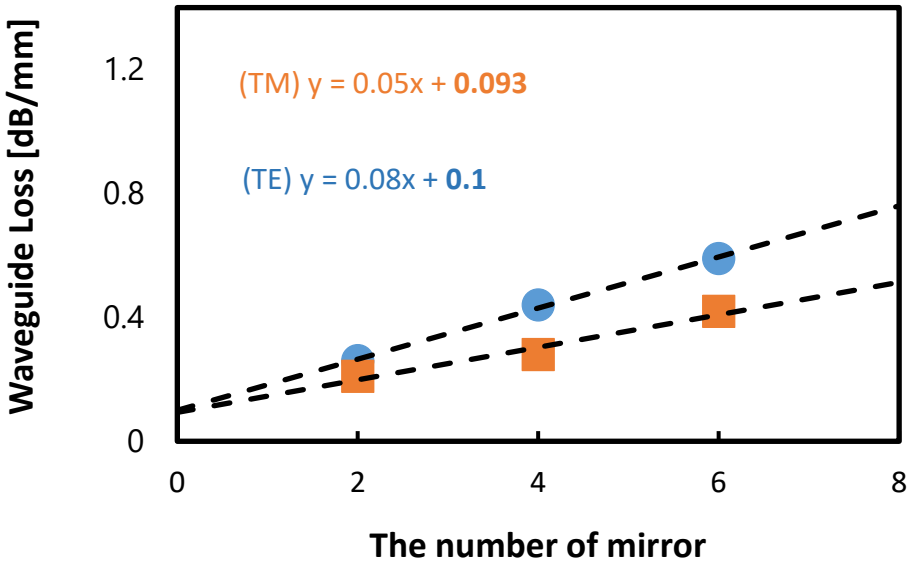

Figure 32. The dependence of total loss after subtracted by the coupling on the number of mirror.

The propagation length of light at each mirror was 24 μm. The distances between mirrors are 50 μm, 100 μm and 200 μm. Hence, in the slab waveguide with

2 mirrors, that the total waveguide lengths are 148 μm, 248 μm, and 448 μm. By the same calculation, the total waveguide length for slab waveguide with 4 and 6 mirrors are 296 μm and 444 μm, 496 μm and 744 μm, 896 μm and 1344 μm, respectively. From Fig. 7, loss condition at zero waveguide length is the coupling loss value. In TE polarization, the coupling loss values are 21.34 dB, 21.27 dB, and 21.17 dB for slab waveguide with 2, 4, and 6 mirrors, respectively. In TM polarization, the coupling loss values are 9.3 dB, 19.26 dB, and 19.2 dB for slab waveguide with 2, 4, and 6 mirrors, respectively. From Fig. 33, it is found that the total loss increases along with the increases of waveguide length and the number of mirrors.

Furthermore, from the gradient in Fig. 8, the net waveguide losses obtained are 0.10 dB/mm and 0.09 dB/mm for the TE and TM polarizations, respectively. Note that, the net waveguide loss is the loss caused by the light propagation in slab waveguide but excludes the mirror loss. The waveguide loss parameter in eq. 5.2 can be identified as:

$$Waveguide\ Loss = net\ waveguide\ loss\ \times propagation\ length \quad (5.2)$$

Moreover, we can assume that the mirror loss is equal to the total loss subtracted by the coupling loss and the waveguide loss.

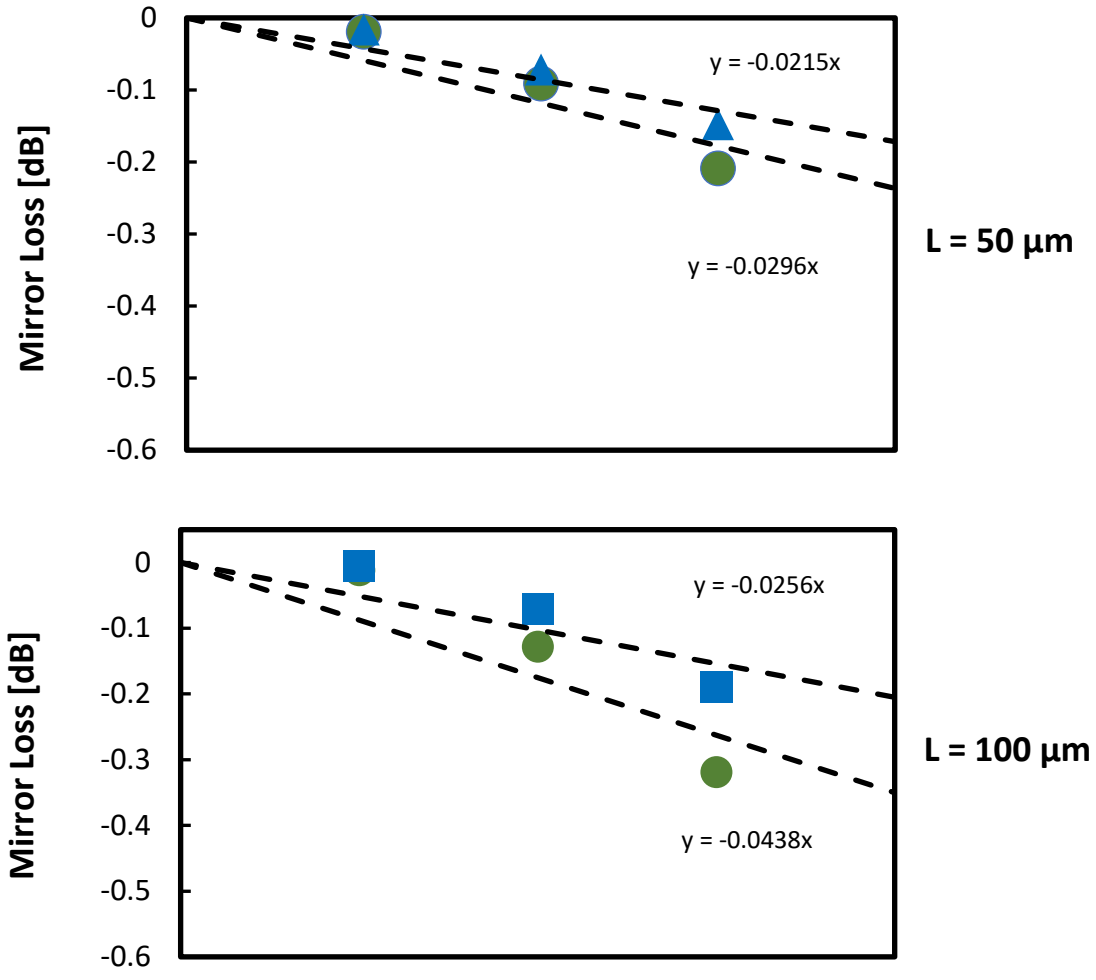

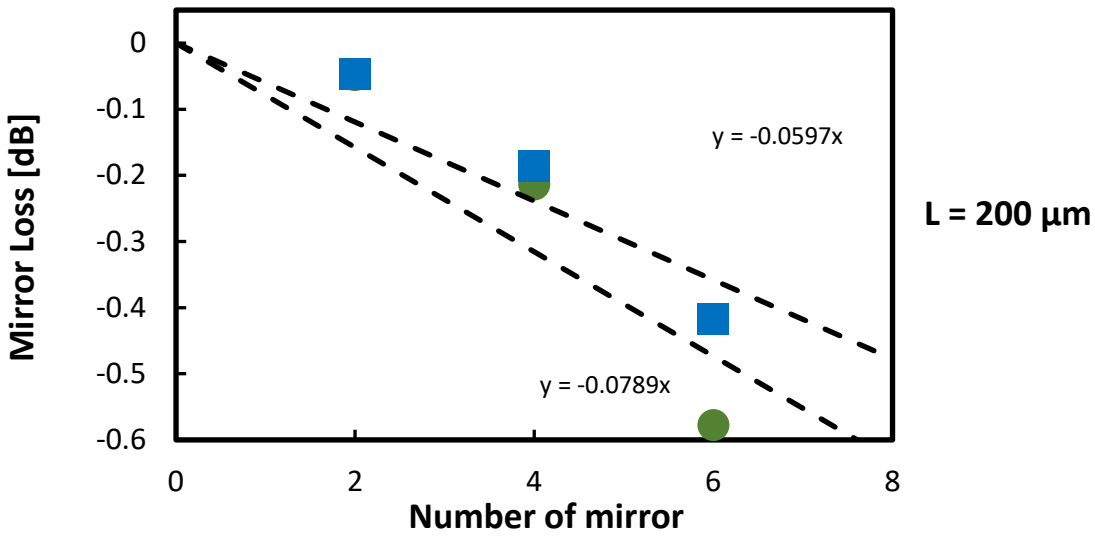

Figure 33. The dependence of the mirror loss on number of mirrors in the slab waveguide. "*L*" is the distance between mirrors, ■ and ● are the TE and TM polarizations, respectively.

The waveguide loss is strongly influenced by the waveguide length so that the calculation of the net waveguide loss must be adjusted. After the net waveguide loss is obtained, the mirror loss is defined. Furthermore, the calculation of the mirror loss which is shown in Fig. 33, does not involve the waveguide length variable anymore. The remaining variable affecting mirror loss is the number of mirrors. Figure 34 shows the mirror

loss value, which is not influenced by the number of the mirror. The linear regression in Fig. 34 should be adjusted to force the mirror loss of zero mirrors to become zero value.

The mirror loss increases while the distance between mirrors becomes longer. This condition is affected by the waveguide loss and mismatch position. The mismatch position might be related to the mirror size and the mirror position. Figure 9 also shows the mirror loss increases in the same trend in 4 and 6 mirrors scenarios. The highest mirror loss occurs while n=6 and L=200μm. The reason for the highest mirror loss is influenced by the waveguide length and the curvature radius of the mirror.

Furthermore, we calculate the average mirror scattering loss on each mirror in the slab waveguide. The average mirror loss is calculated from each value of 2, 4, and 6 mirrors. By the linear regression in Fig. 34, we describe the average mirror loss of each mirror as shown in Fig. 35.

The experimental result of mirror loss has been confirmed by FDTD simulation, in terms of the value and the image of the propagation direction. Based on the simulation, the curved mirror is better than the flat mirror in terms of directing the

light in the slab waveguide. In Figures 4 and 5, it seems that the reflected light of the curved mirror converges, while the reflected light of the flat mirror spreads. The spreading of the reflected light after the first mirror increases the mirror loss at the next mirrors.

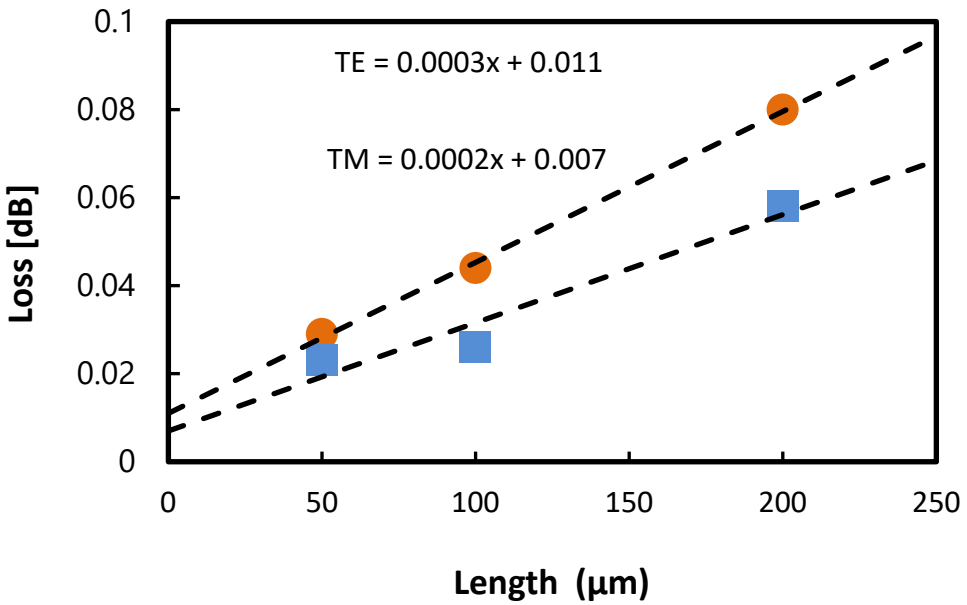

Figure 34. The calculation of the average mirror loss in the slab waveguide.

According to the experimental data, the mirror loss of our slab waveguide is 0.011 dB/mirror and 0.007 dB/mirror for the TE and TM polarizations, respectively. The mirror scattering loss indicates that there is a slight loss on the mirror which might be caused by the imperfection of the slab waveguide design. Both of the TE

and TM polarizations, the results of the calculations give the good tendencies which are proved by the small value of the mirror scattering loss in the slab waveguide.

In the research, the measurement by the FDTD simulation is important to confirm the experimental result. This FDTD simulation also can correct the experimental methods that have been carried out. Besides, the comparison between simulations with experimental results can be used to check the quality of fabricated slab waveguide chips. The FDTD simulation is considered an ideal condition where is no loss due to the defect in the fabrication process.

In the simulation, for calculating the mirror loss, the power monitors are put on before and after the mirror. The monitors' sizes are exactly similar to each other even though the positions of the monitors are horizontal and vertical. In this case, the detected powers indicate power input and power output. The mirror loss calculation follows the Eq. 5.1. The simulation results show the mirror loss is 0.0005 dB and 0.00047 dB for the TE and TM polarizations, respectively. The differences between the simulation results and experimental data may be caused by the imperfections in choosing the size of mesh in *2*-dimension FDTD simulation. The other factor that affecting the mirror loss is the distance between the power

monitor and the mirror because the power monitor and the mirror are not coinciding. However, the tendencies of both results are similar in the TE and TM polarizations.

Chapter 6

Conclusion

We designed the optical slab waveguide included the tapered design, the curve mirror design, and the half-mirror design. And make the hypothesis with the supporting data from the simulation results on these designs. Therefore, these designs can be fabricated in foundry services. After fabrication process, we characterize these design in experiment.

We investigated all properties of propagation loss in our proposed slab waveguide designed with mirror structures. In this analysis, we describe the propagation loss as the total of the coupling loss, waveguide loss, and the mirror loss. The coupling losses at the input and the output ports are the dominant factors in the total loss, but the coupling losses can be reduced by using a lens fiber at the input port. The experimental result of the coupling losses is 21.26 dB and 19.25 dB for the TE and TM polarization, respectively. Furthermore, the waveguide loss is caused by the scattering of the material. The waveguide losses are 0.1 dB/mm and 0.09 dB/mm for the TE and TM polarization, respectively. Moreover, the position

and the size of the mirror also influence the mirror loss. The mirror losses caused by the scattering of the light at the reflection on the mirror are 0.011 dB/mirror and 0.007 dB/mirror for the TE and TM polarizations, respectively. On the other hand, the FDTD simulation results show the waveguide losses are 0.0024 dB/mm and 0.0023 dB/mm for the TE and TM polarizations, respectively. Then, the mirror losses are 0.0005 dB/mirror and 0.00047 dB/mirror for the TE and TM polarizations, respectively. The TE polarization is commonly used in the optical waveguide measurement. However, based on these results, the TM polarization can also be used for giving a similar result. From all the results, we conclude that our design can be applied.

For the future development, the new integrated design that has been fabricated will be characterized by the experiment. The new integrated design is consisting of the several designs such as taper design, mirror design, half-mirror design and retroreflector design. In this new integrated design, a mirror size has been change to be larger. Moreover, it is hoped that this improvement can reduce mirror coupling loss in a system.

References

1) R. N. Noyce, “Large Scale Integration: What Is Yet to Come?”, Science. **195**, pp. 1102-1106, (1977).
2) R. Ulrich and R. J. Martin, “Geometrical Optics in Thin Film Light Guides”, Appl. Optics. **10**, pp. 2077-2085, (1971).
3) J. T. Boyd, R. W. Wu, D. E . Zelmon, A. Naumaan, H. A. Timlin and H. E. Jackson, Proc. SPIE, **517**, pp. 100-105 (1985).
4) X. Zheng and A. V. Krishnamoorthy, “Si Photonics Technology for Future Optical Interconnection”, *Asia Communications and Photonics Conference and Exhibition (ACP)*, 2011, pp. 1-11.
5) P. J. Bock, P. Cheben, J. H. Schmid, J. Lapointe, A. Delâge, X. Dan-Xia, S. Janz, A. Densmore and T. J. Hall, “Subwavelength grating crossings for silicon wire waveguides”, Opt. Express. **17**, pp. 16146-16155, (2009).
6) A. M. Scheggi, R. Falciai and M. Brenci, “Radiation Characteristics of Tapered Slab Waveguides”, J. Opt. Soc. Am. **73**, pp. 119-121, (1983).
7) S. Dwari, A. Chakraborty and S. Sanyal, “Analysis of Linear Tapered Waveguide by Two Approaches”, Prog. Electromagn. Res. **64**, pp. 219-238, (2006).

8) P. Bienstman, S. Aseffa, S. G. Johnson, J. D. Joannopoulos, G. S. Petrich and L. A. Kolodziejski, “Taper structures for Coupling into Photonic Crystal Slab Waveguides”, J. Opt. Soc. Am. **20**, pp. 1817-1821, (2003).

9) J. H. Karp, E. J. Tremblay and J. E. Ford, “Planar Micro-Optic Solar Concentrator”, Opt. Express. **18**, pp. 1122-1133, (2010).

10) H. R. Stuart, “Waveguide Lenses with Multimode Interference for Low-Loss Slab Waveguide”, Opt. Lett. **28**, pp. 2141-3143, (2003).

11) S. Misawa, M. Aoki, S. Fujita, A. Takaura, T. Kihara, K. Yokomori and H. Funato, “Focusing Waveguide Mirror with a Tapered Edge”, Appl. Optics. **33**, pp. 3365-3370, (1994).

12) R. Rogozinski, Planar Gradient Tapered waveguide in Glass”, Opto-Electron Rev. **9**, pp. 326-330, (2001).

13) T. Saastamoinen, M. Kuittinen, P. Vahimaa and J. Turunen, “Focusing of Partially Coherent Light into Planar waveguides”, Opt. Express. **12**, pp. 4511-4522, (2004).

14) S. Wiechmann, H. J. Heider and J. Műller, “Analysis and Design of Integrated Optical Mirrors in Planar Waveguide Technology”,J. Lightwave Technol. **21**, pp. 1584-1591, (2003).

15) M. Hammer, A. Hildebrandt and J. Förstner, “Full Resonant Transmission of

Semi-Guided Planar waves through Slab Waveguide Step at Oblique Incidence", J. Lightwave Technol. **34**, pp. 997-1005, (2016).

16) M. Hammer, A. Hildebrandt and J. Förstner, "How Planar Optical waves can be Made to Climb Dielectric Steps", Opt. Lett. **40**, pp. 3711-3714, (2015).

17) S. Changwan, K. Byungchae, S. Jaehyuk and N. Dagli, "Very Compact Metal Slab Waveguide Reflectors as Integrated High Reflectivity Mirrors on High Index Contrast Waveguides", J. Lightwave Technol. **29**, pp. 2999-3003, (2011).

18) S. T. Lau, T. Shiraishi, P. R. McIsaac, A**.** Behfar-Rad and J. M. Ballantyne, "Reflection and Transmission of a Dielectric Waveguide Mirror", J. Lightwave Technol. **10**, pp. 634-643, (1992).

19) K. Watanabe, J. Schrauwen, A. Leinse, D. V. Thourhout, R. Heideman and R. Baets, "Total Reflection Mirror Fabricated on Silica Waveguides with Focused Ion Beam". Electron. Lett., **45**, pp. 883-884, (2009).

20) K. Jin-Ha and R. T. Chen, "A Collimation Mirror in Polymeric Planar Waveguide Formed by Reactive Ion Etching", IEEE Photonic Tech. L. **15**, pp. 422-424, (2003).

21) K. Tsukamoto, A. Sugama, Y. Wakino, T. Miyashita and M. Kato, "Simple Micro-Lens with Polymer-Filled Trench in Slab Waveguide", Fujitsu Sci. Tech. J. **38**, pp

54-63, (2002).

22) L. Faustini, C. Coriasso, A. Stano, C. Cacciatore and D. Campi, “Loss Analysis and Interference Effect in Semiconductor Integrated WaveguideTurning Mirrors”, IEEE Photonic Tech. L. **8**, pp. 1355-1357, (1996).

23) F. J. Schműckle and R. Pregla, “The Method of Lines for the Analysis of Lossy Planar Waveguides”, IEEE T. Microw. Theory and Tech. **38**, pp. 1473-1479, (1990).

24) M. R. Ramadas, E. Garmire, A. K. Ghatak, K. Thyagarajan and M. R. Shenoy, “Analysis of Absorbing and Leaky Planar Waveguides: A Novel Method”, Opt. Lett. **14**, pp. 376-378, (1989).

25) M. Kawachi, “Silica Waveguides on Silicon and Ttheir Application to Integrated-Optic Components”, Opt. Quant. Electron. **22**, pp. 391-416, (1990).

26) J. F. Bauterst, M. J. R. Heck, D. D. John, J. S. Barton, C. M. Bruinink, A. Leinse, R. G. Heideman, D. J. Blumenthal and J. E. Bowers, Planar Waveguides with less than 0.1 dB/m Propagation Loss Fabricated with Wafer Bonding”, Opt. Express. **19**, pp. 24090-240101, (2011).

27) J. J. Ackert, K. J. Murray, P. E. Jessop and A. P. Knights, “Photodetector for 1550nm Formed in Silicon-On-Insulator Slab Waveguide”, Electron. Lett. **48**, pp.

1148–1150 (2012).

28) B. D. Jennings, D. McCloskey, J. J. Gough, T. Hoang, N. Abadía, C. Zhong, E. Karademir, A. L. Bradley and J. F. Donegan, “Characterisation of Multi-Mode Propagation in Silicon Nitride Slab Waveguide”, J. Opt-UK, **19**, pp. 1-10, (2017).

29) R. Ramponi, R. Osellame and M. Marangoni, “Two Straightforward Methods for the Measurement of Optical Losses in Planar Waveguides”, Rev. Sci. Instrum. **73**, pp. 1117-1120, (2002).

30) Y. Okamura, S. Yoshinaka and S. Yamamoto, “Measuring Mode Propagation Losses of Integrated Optical waveguides: A Simple method”, Appl. Optics. **22**, pp. 3892-3894, (1983).

31) T. Feuchter and C. Thirstrup, “High Precision Planar Waveguide Propagation Loss Measurement Technique Using a Fabry-Perot Cavity”, IEEE Photonic Tech. L. **6**, pp. 1244-1247, (1994).

32) A. Boudrioua and J. C. Loulergue, “New Approach for Loss Measurements in Optical Planar Waveguides”, Opt. Commun. **137**, pp. 37-40 (1997).

33) Y. Morimoto and T. Ishigure, Low-Loss Light Coupling with Graded-Index Core Polymer Optical Waveguides via 45-degree Mirrors”, Opt. Express, **24**, pp. 3550-3561, (2016).

34) Y. Morimoto, R. Kinoshita, A. Takahashi and T. Ishigure,"45-degree Mirrors on Graded-Index cor Polymer Optical Waveguides for Low-Loss Light Coupling", *IEEE Photonics Conference*, 2014, pp. 48-49.

35) Y. Z. Tang, W. H. Wang, T. Li and Y. L. Wang, Integrated Waveguide Turning Mirror in Silicon-on-Insulator", IEEE Photonic Tech. L. **14**, pp. 68-70, (2002).

36) W. A. Challener, C. Mihalcea, C. Peng and K. Pelhos, "miniature Planar Solid Immersion with Focused Spot less than a Quarter Wavelength", Opt. Express. **13**, pp. 7189-7197, (2005).

37) R. Orobtchouk, S. Laval, D. Pascal and A. Koster. "Analysis of Integrated Optical Waveguide Mirrors", J. Lightwave Technol. **15**, pp. 815-820, (1997).

38) F. P. Schäfer, "Dye Lasers", Springer, (1990)

39) F. J. Duarte and L. W. Hillman," Dye Laser Principles", Academic, (1990)

40) Hänsch, T. W. "Repetitively Pulsed Tunable Dye Laser for High Resolution Spectroscopy". Appl. Opt. **11** (4), pp. 895–898. (1972).

41) F. J. Duarte, "Tunable Laser Optics", 2nd Ed. (CRC, New York, 2015) Chapter 7.

42) L. A. Coldren and S. W. Corzine, "Diode Lasers and Photonic Integrated Circuits". New York: Wiley, (1995).

43) M. C. Amann and J. Buus, "Tunable Laser Diodes". London: Artech, 1998.

List of the publication

1. Wildan Panji Tresna, Ryohei Tsurita and Takeo maruyama “Losses Investigating of the Si Optical Slab Waveguide”, *The 6thEM-Nano conference*, P03-40, Aossa-Fukui, 18-21 June, 2017.
2. Wildan Panji Tresna, Takuma Ichikawa and Takeo Maruyama “Waveguide losses and Mirror losses in Si Optical Slab Waveguide “, *The 65th JSAP spring meeting*, 20a-P2-12, Waseda Univ. 17-20 March, 2018.
3. Wildan Panji Tresna and Takeo Maruyama “Reflections of the Optical Si Slab Waveguide: Polarization Dependent”, *IEICE Society 2018*, C-3-3, Kanazawa Univ. 11-14 September, 2018.
4. Wildan Panji Tresna and takeo Maruyama, “Investigation of Mirror losses in Si Optical Slab Waveguide” *IEICE General conference 2019,* C-3-44, Waseda univ. 19-22 March, 2019.
5. Wildan Panji and Taeko Maruyama, “Half-Mirror on the Silicon Slab Waveguide“ *The 80th JSAP conference 2019*, 19a-E206-1, Hokkaido Univ. 10-13 September. 2019.
6. The journal is submitted on the MDPI Photonics journal “Optical Properties of the Si-Slab Waveguide“

Appendix

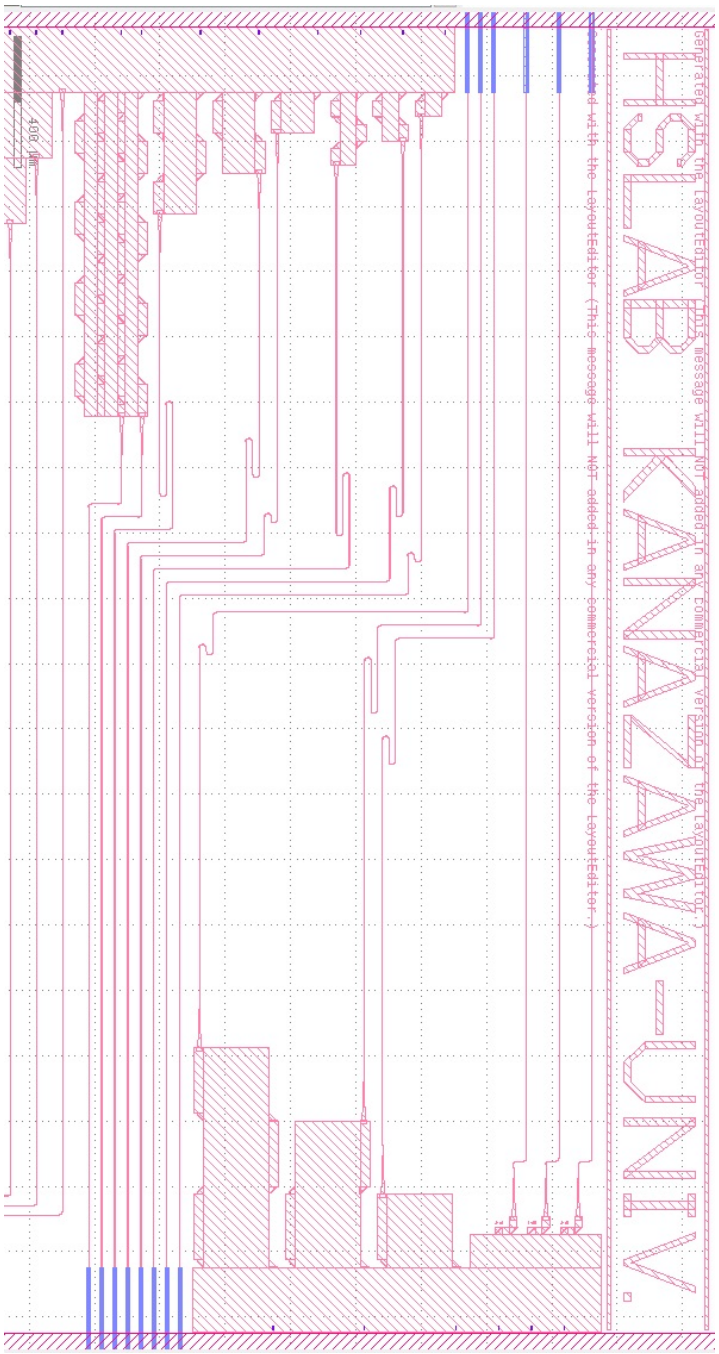

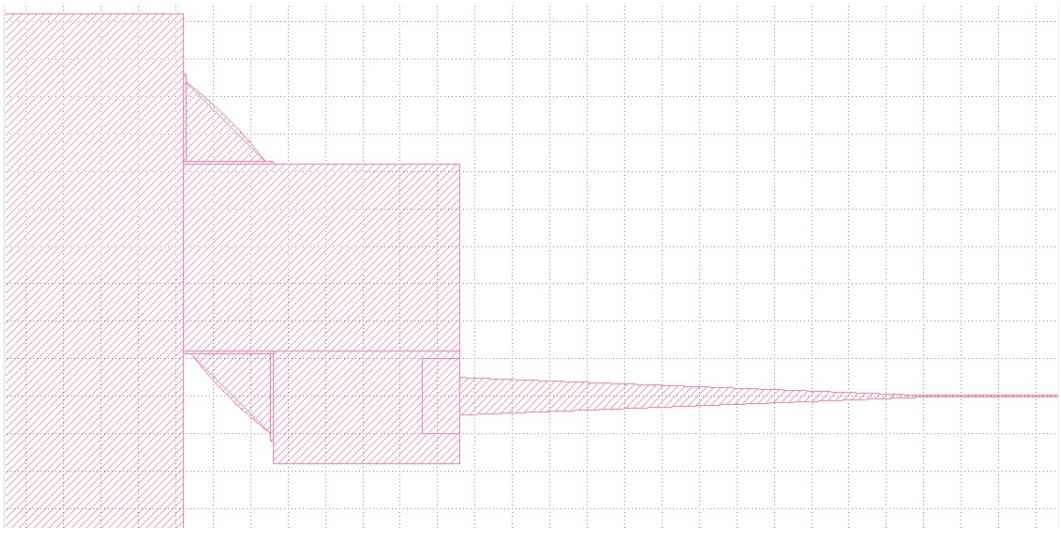

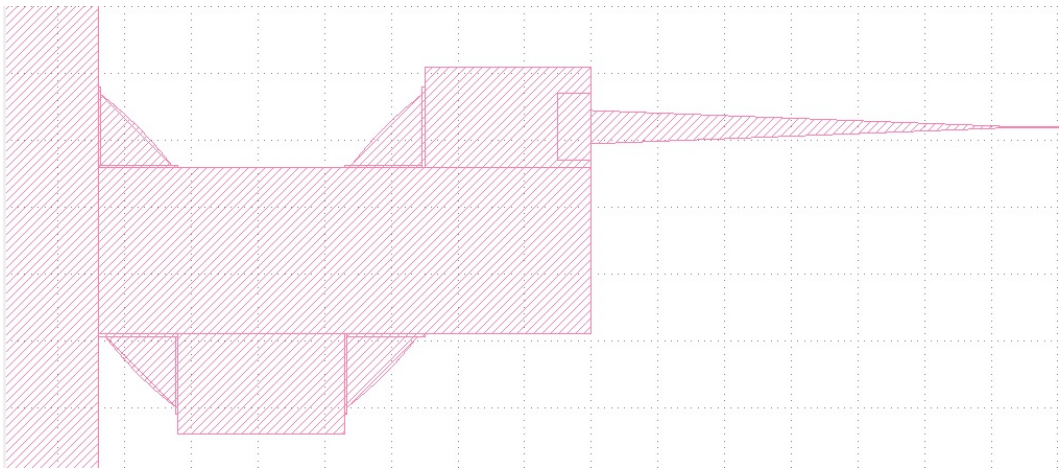

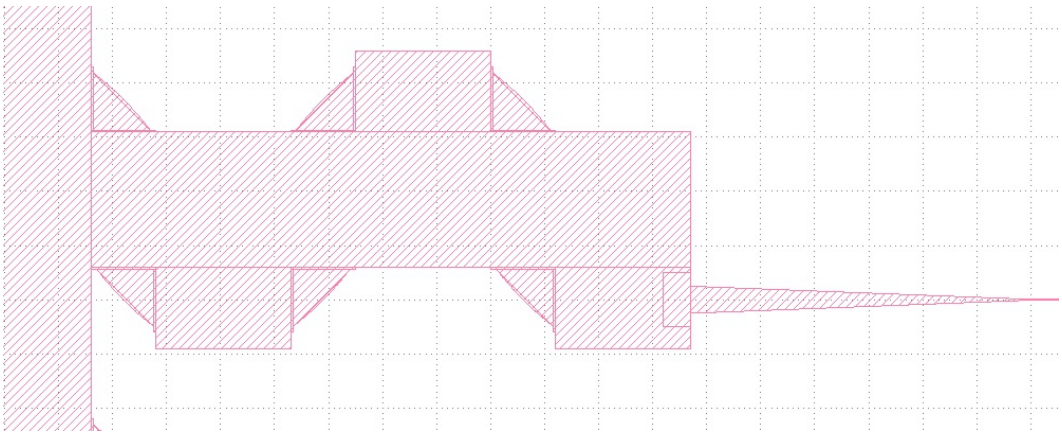

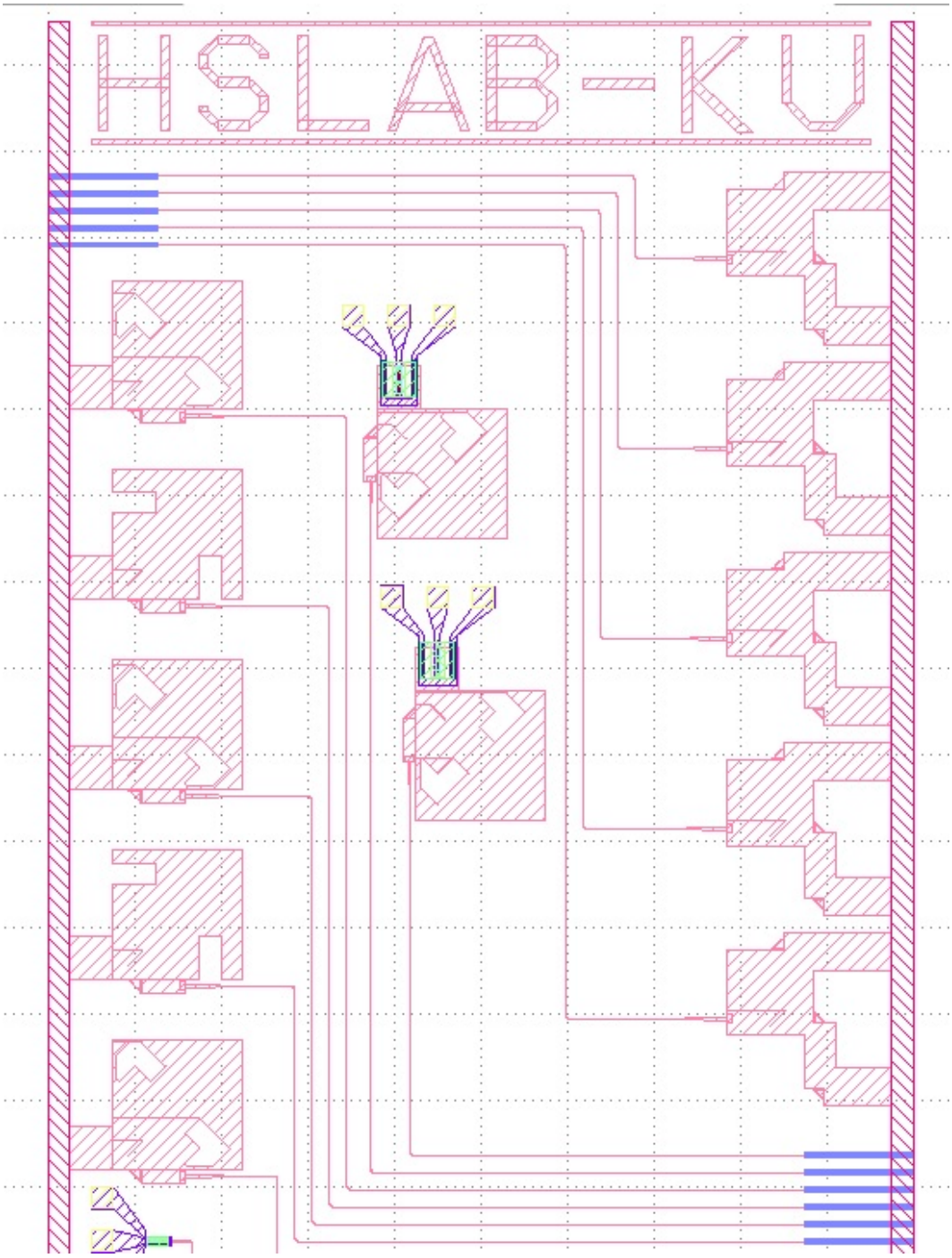
HSLAB-KU